Enhanced Detection of Minispare Usage

Isabella Hansen

Johanna Wikström

LUND
UNIVERSITY

Department of Automatic Control

MSc Thesis
TFRT-6145
ISSN 0280-5316

Department of Automatic Control
Lund University
Box 118
SE-221 00 LUND
Sweden

Printed in Sweden by Tryckeriet i E-huset
Lund 2021

Abstract

Minispares, or spare wheels, can often cause a lot of problems for the control of the car since it rotates notably faster than normal tyres. This because it is often smaller to reduce weight. When a minispare is used, it needs to be detected for the control system to understand that one tyre is allowed to spin faster compared to the others. If the control system does not know this, it will believe that the wheel is slipping and therefore, slow down the speed of the tyre. This detection must happen fast so that the driving experience is affected as little as possible.

This project consisted of improving an already existing method that BorgWarner currently uses to detect minispare usage. The main goal was to decrease the detection time to enhance the driving experience. To reach this goal, different detection algorithms were created and validated with various tests. The algorithms were all based on estimations of the tyres' velocities which were then compared to the measured velocities. In the end, two algorithms were presented which could detect a minispare usage, and the lack of it, in a satisfactory time.

Acknowledgement

First of all, we would like to thank our supervisor at BorgWarner, Ola Nicklasson, for the support and guidance along the way. Your passion for your work as well as your willingness to always give a helping hand, has been a great inspiration for us. The knowledge and input that you have provided throughout the master thesis has been valuable and pushed us in the right direction.

We would also like to thank Daniel Blom for giving us the opportunity to carry out our master thesis at BorgWarner. You always made sure that we were on the right track and had the supplies needed to succeed. When a problem arose, it was always handled as soon as possible to make our experience the best it could be.

To all the employees in *VDS* that we had the pleasure of meeting during our time at BorgWarner, we would like to say thank you for making us feel welcome in your team. Even though we did not meet every day, it always felt as though we could ask any of you for help and that you were interested in our results. A special thank you to Maria Månsson for helping us with setting up the database for the test cars.

Another great thank you to Tore Hägglund, faculty of Engineering at LTH, for being our supervisor and for your encouragement along the way. Your ability to make us believe in ourselves and to make sure that we felt confident throughout the thesis has been greatly appreciated. You have always been open for discussions and provided great inputs to the questions we have had.

To each and every one of you, thank you!
Isabella Hansen and Johanna Wikström

Contents

List of Abbreviations and Symbols

	Abbreviations
CoG	Centre of gravity
FL	Front left wheel
FR	Front right wheel
RL	Rear left wheel
RR	Rear right wheel

	Symbols
a_x	Longitudinal acceleration - [m/s^2]
a_y	Lateral acceleration - [m/s^2]
C_F	Effective cornering stiffness, front axle - [N/rad]
C_R	Effective cornering stiffness, rear axle - [N/rad]
L_F	Length from centre of gravity to front wheels - [m]
L_R	Length from centre of gravity to rear wheels - [m]
m	Vehicle mass - [kg]
tw_F	Track width front - [m]
tw_R	Track width rear - [m]
v	Velocity vector of chassis centre of gravity - [m/s]
v_{xCoG}	Longitudinal velocity at CoG - [m/s]
v_{yCoG}	Lateral velocity at CoG - [m/s]
v_{xXX}	Longitudinal velocity on wheel XX- [m/s]
v_{yXX}	Lateral velocity on wheel XX- [m/s]
β	Chassis slip angle - [rad]
δ	Wheel steer angle - [rad]
$\dot{\psi}$	Chassis yaw rate - [rad/s]

1

Introduction

1.1 Background

In today's society, vehicle handling behaviour must be predictable to be able to avoid accidents. It is, however, not always consistent in all scenarios since there are some non-linearities in the tyre dynamics. This makes it difficult to predict the behaviour in those cases and they need to be handled in specific ways. One of those cases is when the control unit of the car perceives a tyre as slipping, caused by a higher velocity measured on the wheel compared to the others, which is often due to the tyre losing grip. The control unit will then initiate some type of anti-slip actuation that usually handles the problem satisfactory. However, it causes a problem if the car incorrectly perceives the wheel as slipping when in fact the speed deviation is due to something else, e.g. a minispare being used.

The spare tyre that modern cars are generally equipped with is usually considerably smaller than a regular tyre, therefore it is commonly called minispare. The reason for this is mainly because of the desire to reduce cost and weight. Since the minispare has a smaller radius, it rotates notably faster compared to a regular tyre which causes some problems for the control of the car. One of the issues, as mentioned previously, is that the spare tyre will incorrectly seem to be slipping. To accommodate for this, the minispare will have to be detected and compensated for as early as possible. If not, the driving experience will be poor since the car control systems will try to decrease the wheel speed of the minispare.

1.2 Problem formulation

The thesis has been made in collaboration with BorgWarner Sweden AB and they will be referred to as BorgWarner throughout the report. They currently have a method for detecting tyre size difference on all wheel drive cars, however, it is regarded as a bit too slow, and the long detection time can make the driving experience unpleasant for the driver. This thesis focus is on enhancing the method by

creating a new algorithm, or multiple, for the detection of a minispare usage and if time permits, an estimation of the radius of the wheel as well. The main goal is to decrease the amount of time it takes for the detection so that the driving experience will improve. To be able to create a new algorithm, some different driving scenarios will be investigated, these are

- low and mid speed cornering manoeuvring,
- actual drive torque induced wheel slip,
- high front/rear speed differences during acceleration and braking.

In the above driving situations, the wheel speeds will differ from each other when normal tyres are used. The detection algorithm must not falsely detect a minispare in these situations.

1.3 Method

This thesis will begin with literature studies where the new information will be used to formulate equations that describe the velocity of the wheels. These will then be written as algorithms to later be expanded to include detection of a minispare and, if there is time, deciding the difference in radius compared to the other tyres. The velocity estimations will be based on simple models, e.g a single track model, and steady state assumptions. Another way to approach this problem would be to look at the drive line torque and compare that to the measured wheel speeds. However, this approach will not be researched in this thesis. During the entire work period, tests will be performed with a car that uses BorgWarner's all wheel drive system and current tyre difference size detection. The tests will provide data of the behaviour of the car depending on the use of a minispare and the different positions of said minispare on the car. This data is then used to improve and validate the created algorithms. The methods will both be created and verified in *Matlab*.

1.4 Thesis outline

Chapter 2 will explain the vehicle and tyre dynamics that are important for this thesis while Chapter 3 will provide the models used for the velocity estimations. In Chapter 4 the velocity estimations will be explained and the different tests that were performed are described in Chapter 5. The results from the velocity estimations, using data from the tests, will be shown in Chapter 6. Chapter 7 describes the detection algorithms and the results from them are presented in Chapter 8. Lastly, a discussion and conclusion will be given in Chapter 9. There are many results that are not shown in the main report, these are instead presented in the different Appendices.

2

Vehicle and tyre dynamics

This chapter focuses on explaining the most relevant parts of vehicle dynamics, tyre dynamics, and a simple modelling technique. The reason for this is to be able to fully understand the thesis and the thought behind different decisions and conclusions. Note that everything that is described in this chapter are taken from various sources.

2.1 Vehicle dynamics

Yaw rate

The yaw angle describes the rotation of the vehicle around its z-axis, i.e. the change of the heading direction of the vehicle. Taking the time derivative of this angle gives the angular velocity and is called yaw rate, $\dot{\psi}$ [1]. This rate is positive when turning left and negative when turning right if the vehicle is moving forward. However, if the vehicle is in reverse, one must change the sign to get the actual yaw rate since the wheel velocities are always positive even if the tyres are rolling backwards.

Cornering

Most vehicles can only steer the front wheels while the rear axle is fixed and follows the front with a delay. This results in the axles having different cornering radii while turning [2], an example of this can be seen in Figure 2.1.

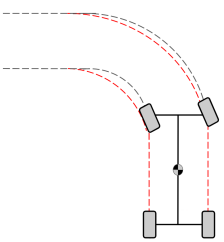

Figure 2.1: The cornering radii for the front (black) and rear (red) wheels

The figure shows that the outer wheels have larger cornering radii compared to the inner ones and therefore, must travel further during the turn. It also illustrates, for low speed cornering, that the front and rear wheels have slightly different cornering radii, with the rear having the largest. All this results in the tyres having different velocities during cornering with the difference between inner and outer wheels being larger than the one between front and rear. The wheel that travels the furthest has the highest speed, in the figure that would be the front right wheel. This phenomenon is the most notable in low speeds, especially the difference in the front and rear wheel velocities. When the vehicle travels at high speed this difference is close to non-existing.

2.2 Tyre dynamics

Radius

In general, a tyre has three different radii. The unloaded radius, R_u, the loaded radius, R_l and the effective rolling radius, R_e, are all illustrated in Figure 2.2. The unloaded and loaded radii are easy to understand by studying the figure. When a tyre rolls on a hard surface, part of the tyre surface is compressed so that the radius is R_l in the first half of the ground contact area and the tyre then expands back to R_u in the other half. To simplify calculations and describe these changes in radius during a rotation of the tyre, a new radius, R_e, is introduced [3].

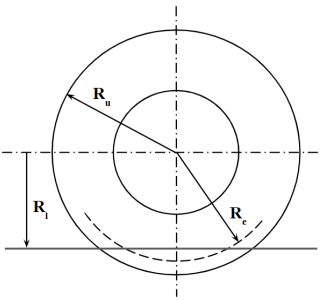

Figure 2.2: A free-rolling tyre with its different radii where the ground surface is shown as a straight line through the bottom of the tyre

Longitudinal and lateral forces

Depending on the driving state and direction of travel, a tyre must withstand forces from multiple axes. In this thesis, the focus is on longitudinal and lateral forces which are the forces along the x-axis respectively y-axis. All the forces that the tyre receives from the road are assumed to be in the centre of the contact patch [4], see Figure 2.3 for illustration.

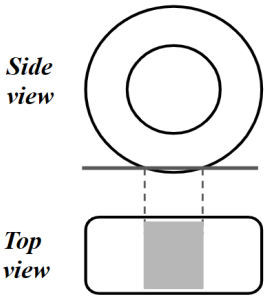

Figure 2.3: The contact patch of a tyre

Pure longitudinal force is generated during acceleration or braking when the vehicle is moving in a straight line, i.e. there must not be a steering angle, $\delta = 0$. This is illustrated in Figure 2.4 where both the ground contact patch and the rim are shown. The direction of $F_{longitudinal}$ depends on if the vehicle is accelerating or braking, however, the velocity, v, will be the same for both cases and only change direction when the car is in reverse. Figure 2.4, therefore, illustrates the scenario when the vehicle is travelling forward and accelerating.

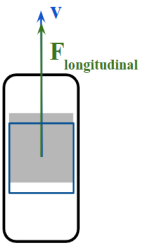

Figure 2.4: Tyre from above where the blue square represents the rim and the grey area is the ground contact area

To generate longitudinal force, as mentioned previously, the driver must either brake or accelerate. This force causes wheel slip and the relationship between the two can be described by longitudinal slip stiffness [5]. In scenarios where $F_{longitudinal}$ is present, the contact patch and the rim are trying to pull the tyre in two different directions, see Figure 2.4. For example, when accelerating from a standstill, the contact patch of the tyre wants to remain in its position while the rim wants to move forward, hence the pulling in different directions and $F_{longitudinal}$ occurs. The opposite applies for braking, i.e. in that case, the contact patch of the tyre wants to continue its movement forward while the rim wants to stand still.

To generate lateral tyre force, the vehicle must not be stationary, i.e. $v > 0$, and the wheel centre line must deviate from the direction of the tyre velocity, see Figure 2.5a. This deviation is called wheel slip angle and is denoted α. For small α, the relationship between it and $F_{lateral}$ is nearly linear and the constant relating them is called cornering stiffness, C_R or C_F [5].

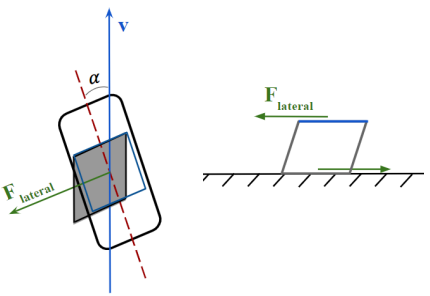

(a) Tyre from above (b) Tyre cross-section

Figure 2.5: The generated $F_{lateral}$ of a rolling tyre, the blue square in (a) and the blue line in (b) represents the rim, and the grey area in (a) is the ground contact area

The generation of lateral force is due to the elastic stiffness properties of the tyre. When a section of the tyre enters the beginning of the ground contact area, it is laterally undeflected. Due to vertical force and friction, the tyre surface in the ground contact area tries to stay in place and thus the orientation of the contact area will be in the direction of the velocity vector, v. On the other hand, the part of the tyre connected to the rim will restrain to remain in contact, see Figure 2.5b where the tyre is shown from behind to illustrate the forces along the y-axis. This causes a lateral deflection of the tyre section as the wheel travels forward since the wheel centre line deviates with an angle, α, compared to the orientation of the ground contact area. The further back in the contact area the more growth in deflection which results in a larger $F_{lateral}$, this is also true for a larger α [5].

2.3 Single track model

The driving dynamic of a vehicle can be described easily without a lot of modelling and parametrisation by using a single track model, also known as the bicycle model. The model approximates the lateral dynamics of the vehicle and is based on a few simplifications, e.g. the vehicle mass, m, is concentrated in the centre of gravity, CoG, at ground level. Both the front and rear wheels are represented as a single tyre on each axle where the attachment points lie along the centre of the axle, this is where lateral tyre forces will arise when cornering [6], see Figure 2.6. The coordinate system and sign convention used in the representation of the vehicle's motion are chosen to the ISO standard [5]. Due to the simplifications, the model has three degrees of freedom. These are the v_x, v_y and the heading angle, ψ, that only occurs as the yaw rate, $\dot{\psi}$. When used for lateral dynamics, v_x is typically given as an input which reduces the degrees of freedom to only v_y and $\dot{\psi}$. The relation between v_x and v_y can be described with the body slip angle, β, depicted in Figure 2.6. It is shown as a negative angle and represents the angular deviation of v_{CoG} from the vehicle's longitudinal direction. The steering angle, δ, and $\dot{\psi}$ are depicted as positive.

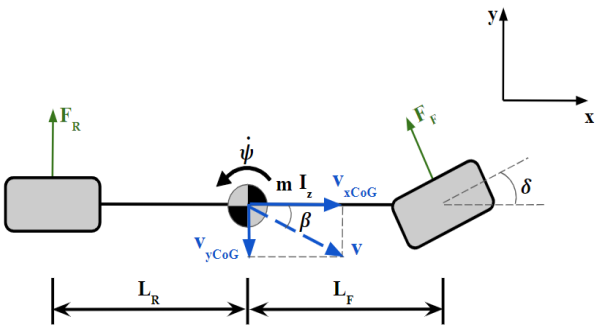

Figure 2.6: The single track model where both β and v_{yCoG} are negative

The lateral tyre forces that are generated while turning can be used to calculate both the yaw acceleration, $\ddot{\psi}$ and the lateral acceleration, $\dot{v}_{yCoG}$ which are described in Equation (2.1).

$$\begin{aligned} I_{zz}\ddot{\psi} = T_z = \cos(\delta)F_F L_F - F_R L_R \approx F_F L_F - F_R L_R \\ m\dot{v}_{yCoG} + m v_{xCoG}\dot{\psi} = \cos(\delta)F_F + F_R \approx F_F + F_R \end{aligned} \tag{2.1}$$

The last step in both expressions is due to small-angle approximation for cosine, Equation (2.2).

$$\cos(\delta) \approx 1 \tag{2.2}$$

Lateral forces

As mentioned in chapter 2.2, when a vehicle turns, lateral forces are generated which can be seen in Figure 2.7, where the cornering circle is shown as a red line.

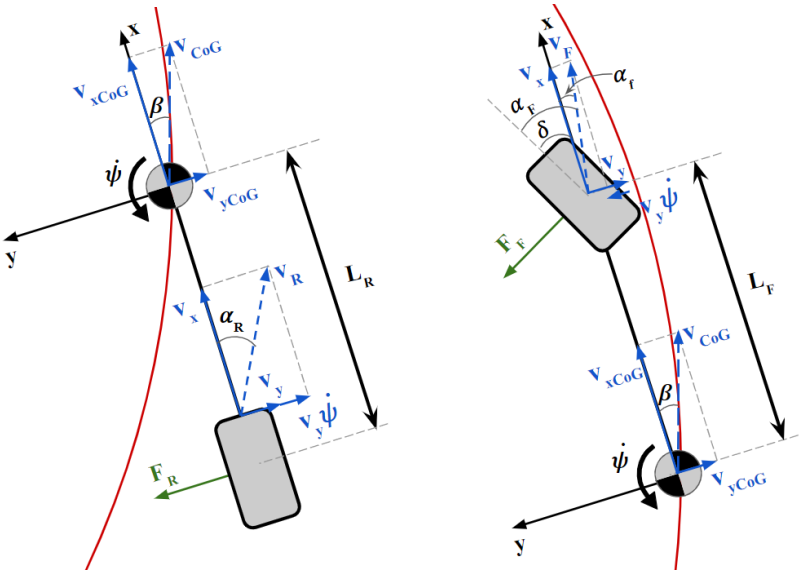

(a) Rear axle (b) Front axle

Figure 2.7: Generated lateral forces on the rear wheel (a) and the front wheel (b) through a curve with a cornering radius (red)

In Figure 2.7a there is an angular displacement, β, between the chassis heading direction, v_{CoG}, and v_{xCoG}. This angle is negative and gives the vehicle body, and thereby the rear tyre, a steering angle towards v_{CoG}, which is needed to generate lateral force. The body slip angle, β, is defined in Equation (2.3).

$$\beta = \tan^{-1}\left(\frac{v_{yCoG}}{v_{xCoG}}\right) \tag{2.3}$$

The rear tyre has the same v_x as the rest of the vehicle since it has no steering angle, however, the tyres v_y is rotated with the positive yaw rate around CoG. It therefore receives an additional component in the negative y-direction, which is illustrated in Figure 2.7a. From this and v_{yCoG}, a slip angle, α_R, for the rear tyre will occur, and together with the cornering stiffness of the rear axle, C_R, results in the lateral force, F_R, described in Equation (2.4) where $v_y\dot{\psi} = -L_R\dot{\psi}$

$$F_R = C_R\alpha_R = C_R\tan^{-1}\left(-\frac{v_{yCoG} - L_R\dot{\psi}}{v_{xCoG}}\right) \approx C_R\left(\frac{L_R\dot{\psi} - v_{yCoG}}{v_{xCoG}}\right) \tag{2.4}$$

Negative v_y generates a positive lateral force which means that α_R is defined as positive for negative v_y. The last step in the equation is due to the use of small-angle approximation for tangent, Equation (2.5).

$$\tan(\delta) \approx \delta \tag{2.5}$$

In Figure 2.7b the attachment point of the front tyre has the same v_x as the rest of the vehicle, however, there is an additional v_y component, similarly as for the rear tyre with the difference that it is in the positive y-direction since the mounting is in front of CoG. Another difference from the rear wheel is that a positive steering angle, δ, is applied, this angle contributes to a negative slip angle, α_F [6]. The angle is illustrated in Figure 2.7b where δ is shown as well. The figure also shows that a positive δ, results in a negative v_y which means that α_F will be negative and the lateral force F_F will be positive. With this information, an expression can be written to describe F_F which is stated in Equation (2.6) where $v_y\dot{\psi} = -L_F\dot{\psi}$.

$$\begin{aligned} F_F = C_F\alpha_F = C_F(\delta + \alpha_f) = C_F(\delta + \tan^{-1}(-\tfrac{v_{yCoG}+L_F\dot{\psi}}{v_{xCoG}})) \\ \approx C_F(\delta - (\tfrac{v_{yCoG}+L_F\dot{\psi}}{v_{xCoG}})) \end{aligned} \tag{2.6}$$

The approximation in the simplification is due to Equation (2.5).

Steady state

The single track model can be assumed to be in a steady state when turning with a fixed cornering radius, which implies that there are no lateral velocity changes, i.e. $\dot{v}_{yCoG} = 0$. There is a yaw torque equilibrium in the steady state, meaning there is no yaw acceleration, $\ddot{\psi} = 0$. These assumptions together with Equation (2.1), (2.4) and (2.6) lead to the following Equation (2.7) and (2.8) [6].

$$I_{zz}\ddot{\psi} = 0 \implies F_F = \frac{L_R}{L_F}F_R \tag{2.7}$$

$$m\dot{v}_{yCoG} = 0 \implies mv_{xCoG}\dot{\psi} = \frac{L_R}{L_F}F_R + F_R = \frac{L}{L_F}F_R = \frac{L}{L_F}C_R(\frac{L_R\dot{\psi} - v_{yCoG}}{v_{xCoG}}) \tag{2.8}$$

Equation (2.8) can be rewritten to describe the ratio between v_{yCoG} and v_{xCoG} as Equation (2.9).

$$\frac{v_{yCoG}}{v_{xCoG}} = \frac{L_R}{v_{xCoG}}\dot{\psi} - \frac{mL_F}{LC_R}v_{xCoG}\dot{\psi} \tag{2.9}$$

3

Modelling

3.1 Two track model

To be able to describe the individual wheel velocities for all four wheels, the single track model needs to be expanded into a two track model which can be seen in Figure 3.1. This expansion leads to there being five degrees of freedom, including the longitudinal and lateral velocities, v_x and v_y, the rotational angles around the x and y-axis, called roll and pitch, as well as the yaw rate, $\dot{\psi}$ [7]. However, to simplify the model, the roll and pitch angles are neglected, reducing the degrees of freedom to three. The mass, m, is still considered to be placed in CoG, but it is no longer located at ground level. Therefore, the mass position differs slightly between different driving scenarios such as acceleration, cornering, and braking due to load transfer. This effect is ignored because of the roll and pitch being neglected.

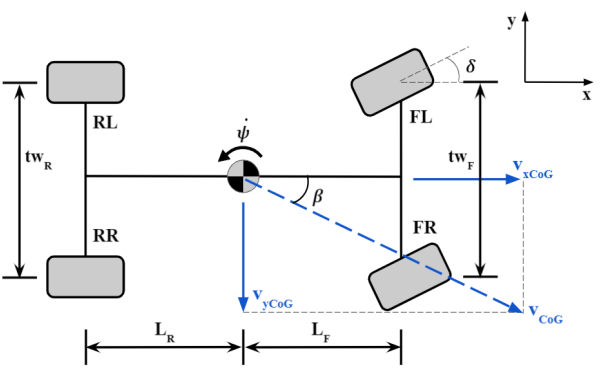

Figure 3.1: The two track model where both v_{yCoG} and β are negative

With the help of the two track model, the individual wheel velocities can be described with different methods.

Velocity estimation from axle velocities

One of the previously mentioned methods is to use the front and rear axle velocities, v_F and v_R. The first step is to describe the hub velocities of the front wheels using the front axle velocity as seen in Equation (3.1). Since there is a displacement on the y-axis for the hub velocities compared to the front axle velocity, an addition of a $\dot{\psi}$ term is needed to fully describe the x components. For the y component, no such term is needed due to there being no difference in the x-axis position.

$$\overset{hub}{v_{FX}} = \begin{bmatrix} \overset{hub}{v_{xFL}} & \overset{hub}{v_{yFL}} \\ \overset{hub}{v_{xFR}} & \overset{hub}{v_{yFR}} \end{bmatrix} = \begin{bmatrix} v_{xF} - \frac{tw_F}{2}\dot{\psi} & v_{yF} \\ v_{xF} + \frac{tw_F}{2}\dot{\psi} & v_{yF} \end{bmatrix} \tag{3.1}$$

While cornering, the front wheels coordinate system will be displaced with the angle δ from to the hubs, which follows the chassis coordinate system. Hence, a rotation matrix relating these two to each other is needed to describe the wheel velocities at all times in their own local coordinate systems. The rotation matrix is stated in Equation (3.2).

$$R = \begin{bmatrix} \cos(\delta) & -\sin(\delta) \\ \sin(\delta) & \cos(\delta) \end{bmatrix} \tag{3.2}$$

By using the rotation matrix, the front wheel velocities can be calculated with Equation (3.3).

$$v_{FX} = \overset{hub}{v_{FX}} R \tag{3.3}$$

This equation results in the velocities being divided into an x and y component. However, the wheels rotational velocities are fully described by their local x component since a tyre only rolls in the x-direction.

The rear wheels are not rotated compared to the hubs, resulting in the velocities being equivalent to the rear hub velocities, which only have an x component. Since there is a displacement in the y-direction compared to the rear axle velocity, an addition of a $\dot{\psi}$ term is needed. From this, the individual wheel velocities can be written as Equation (3.4), where the final expression for the front wheels are also included.

$$v_{XX} = \begin{bmatrix} v_{FL} \\ v_{FR} \\ v_{RL} \\ v_{RR} \end{bmatrix} = \begin{bmatrix} \overset{hub}{v_{xFL}}\cos(\delta) + \overset{hub}{v_{yFL}}\sin(\delta) \\ \overset{hub}{v_{xFR}}\cos(\delta) + \overset{hub}{v_{yFR}}\sin(\delta) \\ v_{xR} - \frac{tw_R}{2}\dot{\psi} \\ v_{xR} + \frac{tw_R}{2}\dot{\psi} \end{bmatrix} \tag{3.4}$$

Velocity estimation from one wheel velocity

Another method to describe the individual wheel speeds is to make use of the vehicle's velocity at the centre of gravity. This can be calculated in many ways, in this instance it is estimated from the rear left respectively rear right wheel velocity. The expressions for the two different v_{xCoG} can be seen in Equation (3.5).

$$\begin{aligned} v_{xCoG} &= v_{RL} + \tfrac{tw_R}{2}\dot{\psi} \\ v_{xCoG} &= v_{RR} - \tfrac{tw_R}{2}\dot{\psi} \end{aligned} \tag{3.5}$$

The y component, v_{yCoG}, can then be described using Equation (2.9) defined in *Steady state* in Chapter 2. With the help of the x and y components, the front wheel hub velocities can be calculated with Equation (3.6).

$$\overset{hub}{v_{FX}} = \begin{bmatrix} \overset{hub}{v_{xFL}} & \overset{hub}{v_{yFL}} \\ \overset{hub}{v_{xFR}} & \overset{hub}{v_{yFR}} \end{bmatrix} = \begin{bmatrix} v_{xCoG} - \frac{tw_F}{2}\dot{\psi} & v_{yCoG} + L_F\dot{\psi} \\ v_{xCoG} + \frac{tw_F}{2}\dot{\psi} & v_{yCoG} + L_F\dot{\psi} \end{bmatrix} \tag{3.6}$$

One thing to note is that the y components have an addition of a $\dot{\psi}$ term in contrast to Equation (3.1). This is because there is a displacement in the x-direction as well, compared to only in the y-direction as for the previous method.

Similarly, to the previously mentioned method, the hub velocities need to be rotated with the matrix in Equation (3.2). Once rotated, the x components fully describe the front wheel velocities in their rotational direction and are seen in Equation (3.7). In the equation, the rear wheel velocities are stated as well, the motivation behind their expression is the same as for Equation (3.4).

$$v_{XX} = \begin{bmatrix} v_{FL} \\ v_{FR} \\ v_{RL} \\ v_{RR} \end{bmatrix} = \begin{bmatrix} \overset{hub}{v_{xFL}}\cos(\delta) + \overset{hub}{v_{yFL}}\sin(\delta) \\ \overset{hub}{v_{xFR}}\cos(\delta) + \overset{hub}{v_{yFR}}\sin(\delta) \\ v_{xCoG} - \frac{tw_R}{2}\dot{\psi} \\ v_{xCoG} + \frac{tw_R}{2}\dot{\psi} \end{bmatrix} \tag{3.7}$$

4

Velocity estimations

With the help of the acquired data, from the tests described in Chapter 5, different algorithms to both detect minispare usage and estimate the radius of the new tyre could be derived. They are all based on some type of comparison between the measured and estimated velocities. In this chapter, a description of how the velocity estimations were done will be given.

To estimate the velocities, some signals from the car are needed together with a few given constants. These signals are listed below, and the constants are stated in Table 4.1.

- a_x, a_y, $\dot{\psi}$, δ
- v_{FL}, v_{FR}, v_{RL}, v_{RR}

The car calculates the velocities by multiplying wheel angular speed, ω, with the radius, R_e, set in the car. The ω is measured while the R_e is fixed, thus, when a smaller tyre is used, ω is correct and R_e is too big, resulting in a too high velocity.

Constant	**XC40**	**XC60**
L_F [m]	1.14	1.40
L_R [m]	1.59	1.46
tw_F [m]	1.60	1.65
tw_R [m]	1.60	1.65
R_e [m]	0.354	0.361
m [kg]	1697	2012
C_R [kN/rad]	120	100

Table 4.1: Constants for the two cars used during tests

4.1 Velocity estimation 1 - Axle velocities

This estimation was done by first estimating the axle velocities to then be able to use them in the method described in *Velocity estimation from axle velocities* in Chapter 3, to calculate the individual wheel speeds. A version of Equation (2.9) was used to estimate the front axle velocity from the measured rear axle velocity and vice versa. However, the axle velocities cannot be measured, hence it was assumed that they were equivalent to the mean value of v_{FL} and v_{FR} for the front and v_{RL} and v_{RR} for the rear axle. Due to a lot of noise regarding the measured wheel speeds, a low-pass filter was implemented as well. It was a butterworth filter and the different parameters were tuned by comparing the filtered velocities to the unfiltered ones.

With this estimation, there should be a specific pattern in the ratios between the estimated and measured velocities during minispare usage. When comparing to the measured wheel speeds when a minispare is placed on one of the front wheels, the rear velocities should be estimated too high, the minispare too low and the other front wheel somewhat correct. The opposite should be true if the minispare is placed on one of the rear wheels. It should also result in the ratio between the estimated and measured minispare velocity being equal to the ratio between the minispare radius and the radius set in the car.

4.2 Velocity estimation 2 - One wheel velocity

In this estimation, the method and equations explained in *Velocity estimation from one wheel velocity* in Chapter 3 was used to estimate the individual wheel speeds. As the method states, the rear wheels are used to estimate v_{xCoG}. This decision was made due to δ being an important factor for the front wheels and thus the expressions would have been more complicated. The final step in this estimation was to implement a low-pass filter on the measured velocities to reduce the noise.

The ratio pattern in this algorithm should be a bit different compared to the previous one. If the rear left velocity is used for estimating all wheels, except for the RL wheel where the rear right velocity is used to estimate the velocity, all estimations should be close to or equal to their respective measured wheel speed except for the one with a minispare, which will be too low. This is if the minispare is placed in any other position than RL. In case of the minispare being placed on RL, all other estimations should be too high and the rear left one too low. The corresponding should be true if the RR velocity is used for estimating the other wheel speeds and the RL velocity is used for estimating the rear right velocity. For both the estimations, the minispare estimation should result in a velocity ratio that is equal to the radius ratio.

5

Tests

All tests have been done with a Volvo XC60 unless something else is stated. The minispare that has been used, has an effective rolling radius of 0.329 m which is an 8.4 % reduction compared to the standard tyres on the car which has an effective rolling radius of 0.359 m.

5.1 Test 1 - City drive

At the beginning of the thesis work, this a city drive test was done to collect data of the vehicles behaviour depending on if a minispare was being used or not and on said minispares position on the car. It consisted of driving a specific route through Landskrona city while five different log files were taken. The idea was to simulate a typical city drive which often has quite a low speed, a lot of turns, and driving in reverse when parking. Even if the reversing part is often very short while driving, it is still important to make sure that the algorithm would make the correct choice. The route was divided into five different parts, part 1-5, where the last part was done in a parking lot, for a map of the route see Figure A.1 in *Appendix A*. Five different scenarios were tested for the route, which is the following:

- Standard tyres (1)
- Minispare on FL (2)
- Minispare on FR (3)
- Minispare on RL (4)
- Minispare on RR (5)

5.2 Test 2 - Ljungbyhed

A second test was done at Ljungbyhed which is a test track that BorgWarner rent when larger tests must be done. The track allows for a lot of tight cornering at high speeds and a few straight distances where you can accelerate fast. Since this test was supposed to be quite a rough drive to create a lot of lateral forces and put the car to a test, our supervisor Ola was in charge of the driving. It was decided that five different tests would be enough to study, these were:

- Tight cornering (Test 2.1)
- High speed (Test 2.2)
- Acceleration (Test 2.3)
- Off road (Test 2.4)
- Fast turns (Test 2.5)

All tests were performed with (1) normal tyres, (2) minispare on FL, and (4) minispare on RL.

Test 2.1 - Tight cornering

The first test was performed by driving aggressively on a part of the test track that allowed for a lot of tight cornering. This meant that there was a lot of hard braking, acceleration, and wheel slip. Because of the rough driving, load transfer was introduced as well, which might negatively impact the detection algorithm. There was also a lap when the driving was calmer to allow for comparison between normal and aggressive driving.

Test 2.2 - High speed

This test was very similar to the previous one with the difference being that it included fewer curves and longer straight distances. Therefore, the velocity was generally higher, the accelerations continued for a longer period and there was an even larger need for hard braking before cornering.

Test 2.3 - Acceleration

The acceleration test was done by forcing longitudinal wheel slip on either the right or left wheels while accelerating. To obtain the wheel slip, the wheels on one side were rolling on asphalt and the others on grass.

Test 2.4 - Off road

To simulate an off road environment, this test was done on an uneven grass field that had a lot of bumps and holes. The driving was mixed, both slow turns and fast tight turns. This was to get the wheels to rotate at different speeds regardless of a minispare usage which could make it harder for the algorithm. The main point of this test was to make sure that the algorithm would not detect any wrongful minispares despite the difficulties that comes with off road driving.

Test 2.5 - Fast turns

This test was performed by driving fast in circles, both clockwise and counterclockwise, to create lateral forces and hence, load transfer.

5.3 Test 3 - City drive with Volvo XC40

The test was identical to *Test 1 - City drive* with the exception that a Volvo XC40 was used instead which had smaller standard tyres compared to the XC60. The effective rolling radius of these wheels was 0.347 m which is 5.3 % larger than the minispare. The reason for testing this was to see if the algorithm could detect a smaller difference between the standard and smaller tyre. Since this test was only performed to validate the algorithms for a bigger minispare, and no changes were made due to it, no figures or tables will be shown in the report, however, they can be found in *Appendix D*. The results from the test will still be discussed in Chapter 9.

6

Velocity Estimation Results

In this chapter, figures of the collected data from Test 1 and 2 described in Chapter 5, will be presented as well as the velocity estimations. The reason for not showing the results from Test 3 is that it did not provide any new behaviour compared to the previous ones, these can instead be found in *Appendix D*. To process the data, the two estimations, mentioned in Chapter 4, will be used. This is to then be able to analyse the two methods as well as compare the estimated velocities to the measured ones. Note that ratios will be used to make the comparisons and are always calculated by estimated velocity divided by measured velocity.

The sections in this chapter will be focused on one test and one estimation each to be able to give a thorough description and explanation of the behaviour in the figures regarding that specific test. Many of the test cases behave similarly, therefore, to reduce the heaviness of the report, only a selected number of cases are described. All the ratios for the remaining cases and the tests that are not presented can be found in *Appendix B* for Test 1 and *Appendix C* for Test 2.

6.1 Test 1 - City drive with Velocity estimation 1

Figures of part 1, 3, and 5 from *Test 1 - City Drive* with two cases, standard wheels and minispare on front left, will be presented in this section. These parts were chosen to show the estimation performance in outer city driving, part 1, city core driving, part 3, and slow parking lot driving, part 5. The top left graph of each figure corresponds to the measured velocities while the top right shows the estimated velocities and the bottom one represents the ratio between the two, calculated with estimated divided by measured. In this entire section, the estimations have been derived with the help of Velocity estimation 1, which uses the axle velocities for the calculations and is described in Section 4.1.

Standard tyres

The graphs illustrating the measured velocities in Figure 6.1 and 6.2 shows that the wheel speeds are often roughly the same when normal tyres are used. However, there are some parts where they differ and, in this case, it is due to cornering, which corresponds to the vehicle dynamics mentioned in Chapter 2. This cornering effect is more visible in Figure 6.3 where it is clearly seen that the front wheels rotate faster than the rear and the inner wheels are slower than the outer. Another thing to note in the figures is that both part 3 and 5 include some reversing in the beginning which is not encompassed in part 1.

When comparing the three estimated velocity graphs to their measured counterpart, they all seem to be similar. With the help of the ratio, this can be confirmed since the error is between ± 2 % during most of the time, even though it can be seen that the estimations are slightly worse during cornering. The ratio plot in Figure 6.2 is not as stable as the other ones, especially around time 250, this is due to driving on cobblestone and not only asphalt in part 3.

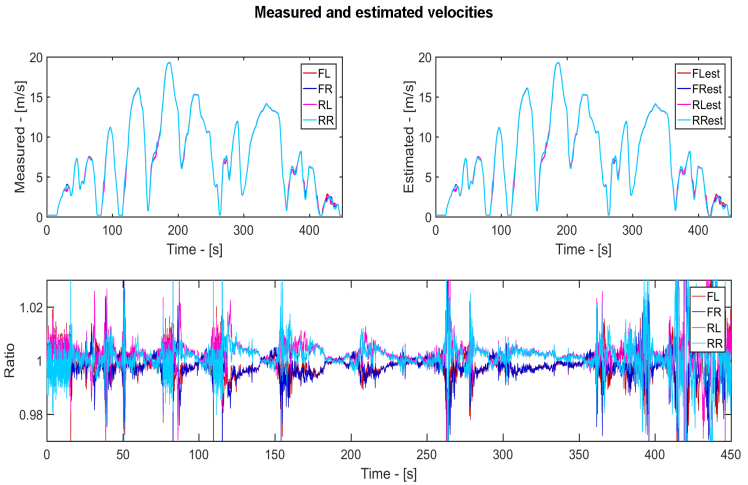

Figure 6.1: Processed data from part 1 of Test 1 with normal tyres

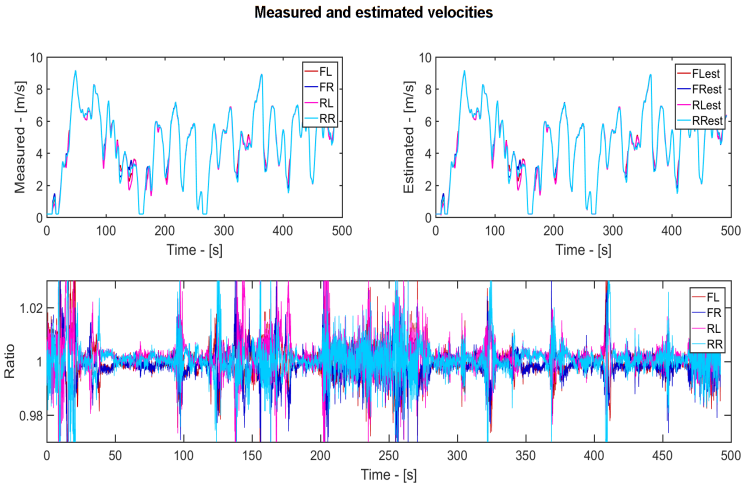

Figure 6.2: Processed data from part 3 of Test 1 with normal tyres

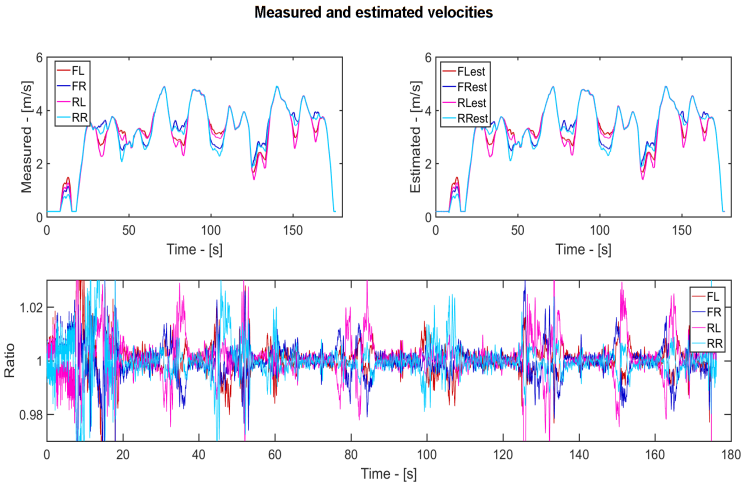

Figure 6.3: Processed data from part 5 of Test 1 with normal tyres

Minispare on front left

Figure 6.4, 6.5, and 6.6 look different in contrast to the ones with normal wheels. In the measured velocity graphs, the front wheel has a higher speed compared to the others which is expected, since the minispare is placed in that position. The estimations are not as accurate in this case which can be seen in both the estimation and ratio plots. They show that the rear wheel velocities are estimated too high and FL too low. This is an anticipated result considering that Velocity estimation 1, see Section 4.1, has been used.

The figures all follow the same ratio pattern, even though they represent different city driving cases. Because of this, the velocity estimation can be deemed as stable and good enough to handle all types of city driving. The pattern can be seen for the other parts and with a minispare on different positions in *Appendix B*.

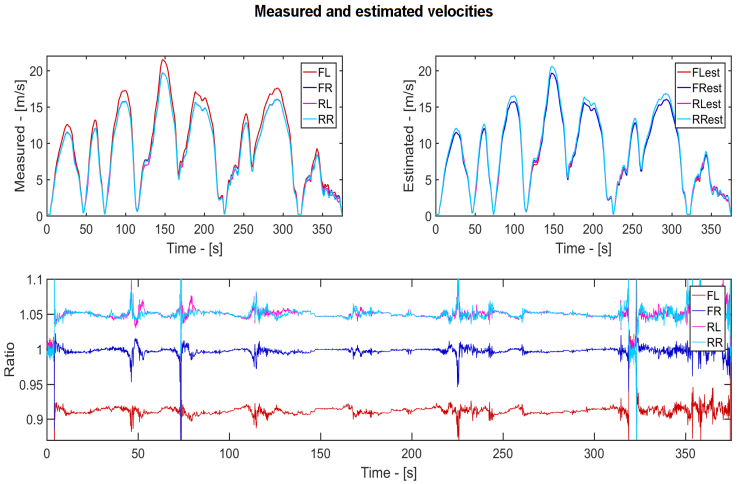

Figure 6.4: Processed data from part 1 of Test 1 with minispare on FL

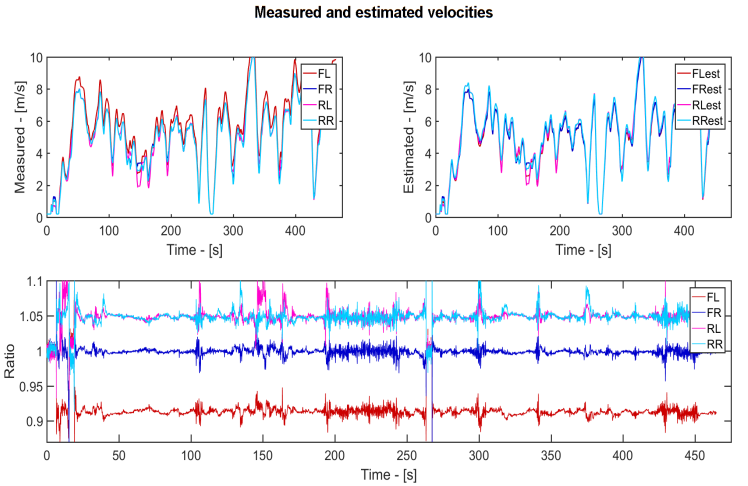

Figure 6.5: Processed data from part 3 of Test 1 with minispare on FL

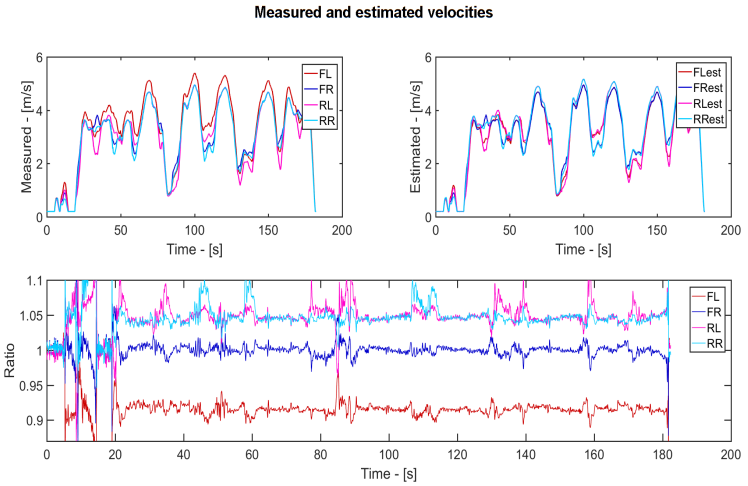

Figure 6.6: Processed data from part 5 of Test 1 with minispare on FL

6.2 Test 1 - City drive with Velocity estimation 2

In this section, the estimations have been calculated with the help of Velocity estimation 2, which uses one wheel velocity as described in Section 4.2. The same test as in the previous section will be discussed, therefore, the same driving scenarios will be presented. However, the case with normal tyres will not be shown, this is because it does not provide any new information. The estimations, in that case, are close to the measured velocities. This can be seen in Figure 6.10, 6.11, and 6.12 where the ratio for normal tyres is shown. The figures showing the remaining ratios between estimated and measured velocities can be found in *Appendix B*.

The test cases that will be presented in this section are minispare on front left for part 1 and minispare on rear left for both part 3 and 5. The reason for this will be explained further down when the errors are presented.

Velocity estimations

The following figures, Figure 6.7, 6.8, and 6.9, show the measured and estimated velocities for each position on the car. In Figure 6.7, which shows a minispare on front left, it can be seen that the estimations for all tyres follow the measured velocity well except FL which is a bit too low. For Figure 6.8 and 6.9 another behaviour can be observed, namely that the estimations are too high for those wheels that have a normal tyre and too low for RL. These behaviours prove that the expectations regarding the behaviour as stated in Section 4.2 were correct.

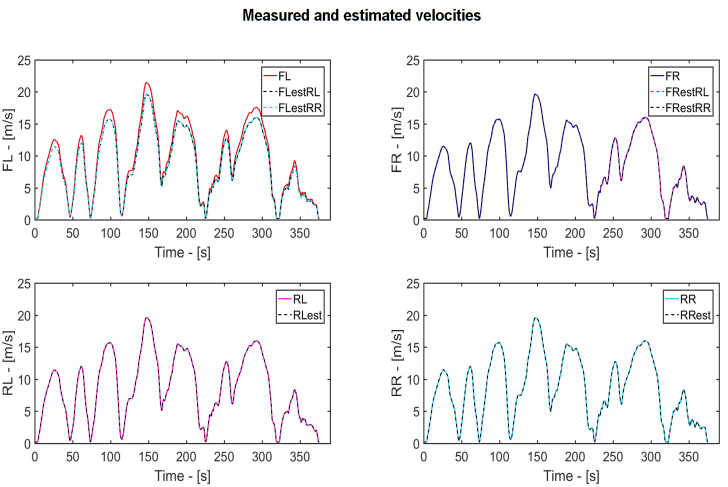

Figure 6.7: Processed data from part 1 of Test 1 with minispare on FL

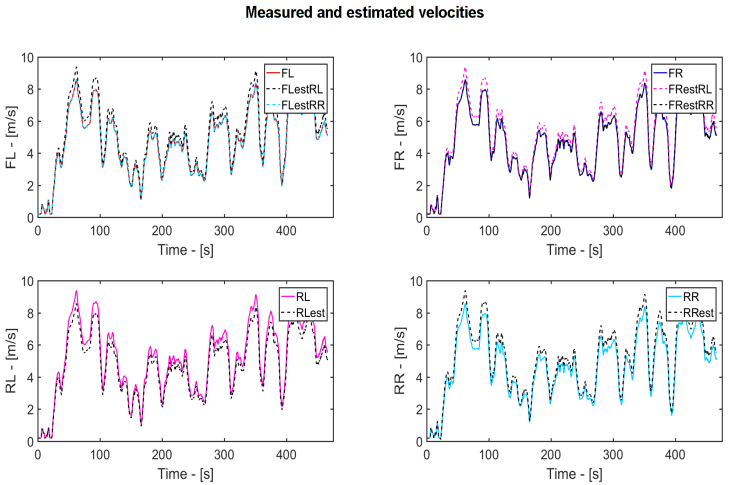

Figure 6.8: Processed data from part 3 of Test 1 with minispare on RL

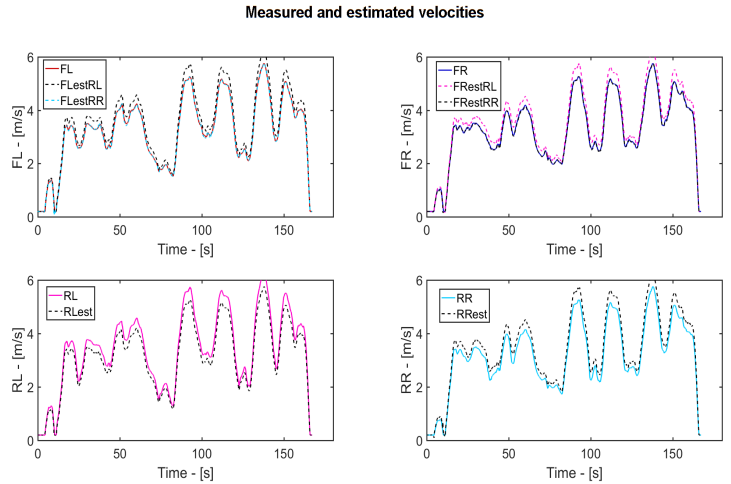

Figure 6.9: Processed data from part 5 of Test 1 with minispare on RL

Ratio

In Figure 6.10, 6.11, and 6.12 below, the ratio between measured and estimated velocities for the different wheels is presented. The estimations, regardless if done from rear left or rear right, are almost identical when a minispare is not located on the rear wheels, refer to Figure 6.7. Because of this, only the ratios when estimating from RL will be shown, except for the rear left ratio that uses the estimation from RR. The top graph in all three figures shows the ratio when normal tyres are being used and the bottom is when a minispare is being used in one position. The bottom graph in Figure 6.10 represents part 1 with the minispare on FL, in the graph, it can be seen that three of the ratios are in an interval of ± 2 % while the one for front left is a lot lower. Since the estimations shown in the previous figures all followed the measured velocities well except for FL, this behaviour was anticipated.

When it comes to the bottom graph in Figure 6.11 and 6.12, which shows part 3 and 5 with the minispare on RL, it can be seen that the ratio for the normal tyres are quite high. On the other hand, the ratio for RL is well below 0.95. This is expected considering the previous figures of the measured and estimated velocities, which showed that the estimations were too high for the normal tyres and too low for RL.

The behaviour for these figures confirms that the expected pattern for the ratio described in Section 4.2 was true. Therefore, it can be said that this pattern is true for the remaining cases for *Test 1 - City drive*.

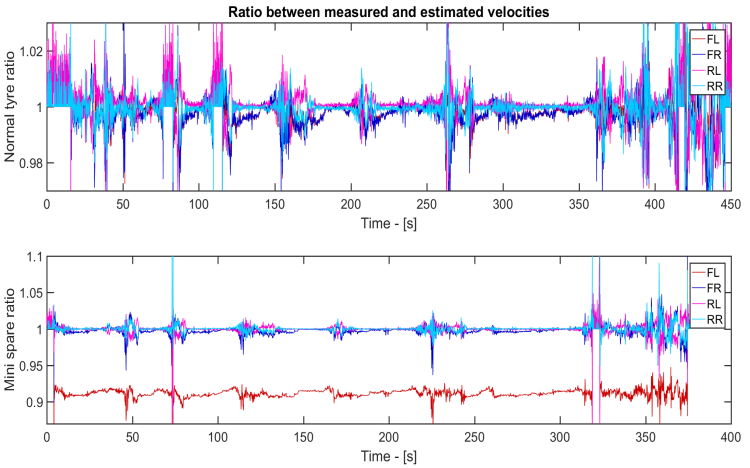

Figure 6.10: Ratio for Test 1 during part 1 for normal tyres and minispare on FL

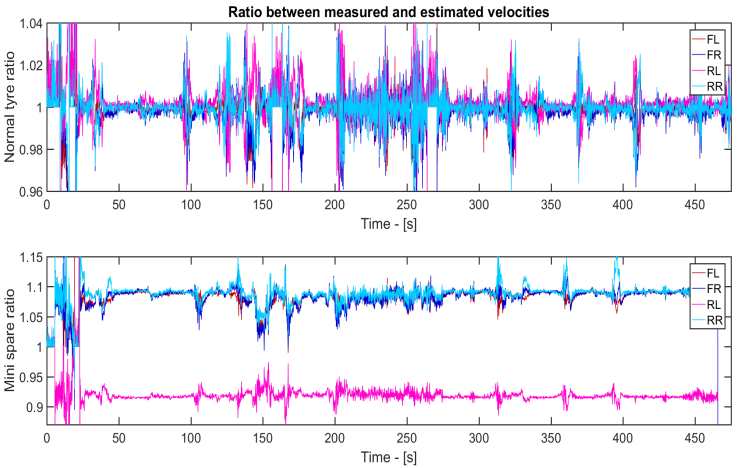

Figure 6.11: Ratio for Test 1 during part 3 for normal tyres and minispare on RL

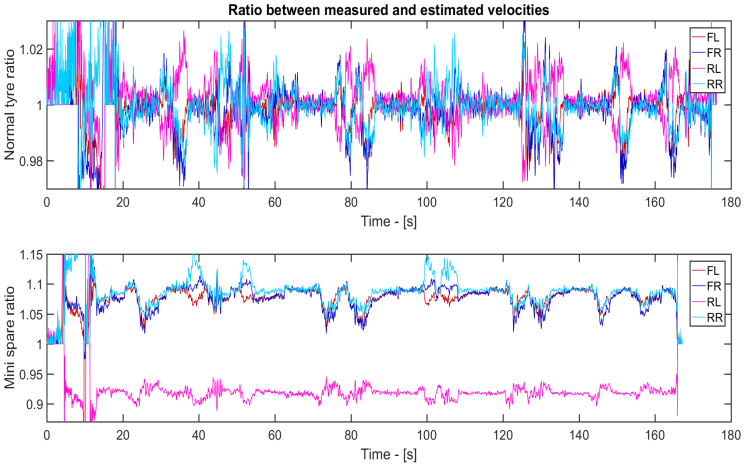

Figure 6.12: Ratio for Test 1 during part 5 for normal tyres and minispare on RL

6.3 Test 2 - Ljungbyhed with Velocity estimation 1

The following figures in this section represent *Test 2 - Ljungbyhed* when Velocity estimation 1 has been used for the estimations. All test cases, Test 2.1-2.5, will be presented, however, it will only be shown with normal tyres and minispare on FL. This is because, with the help from Section 6.1, the pattern for the ratios that were predicted in Section 4.1, has been proved to be correct. The ratios for when a minispare on rear left is used can be found in *Appendix C*.

In every figure, the top left graph illustrates the measured velocities for all tyres while the top right shows the estimated ones. The bottom graph represents the ratio between the two, where the ratio is calculated by estimated velocity divided by measured. Many of the normal tyre velocity plots will look different compared to the ones presented in Section 6.1. This is because these tests were done to create lateral and longitudinal forces and put the car to a test, where lateral and longitudinal tyre slip stiffness reaches non-linear ranges, and thereby can affect the wheel velocity estimations. All this meant that the driving had to be quite rough. Because of this, the estimations will be a bit off at times since they do not take changes in longitudinal forces, or excessive lateral forces into account. The ratios will, therefore, be less smooth compared to those presented in Section 6.1. However, comparing the ratios for normal tyres to the ones for minispare on FL, a significant difference can still be seen. This means that by looking at the ratios, it will be possible to see if a minispare is used or not even in worst case scenarios like these.

The test cases will be presented in the same order as in Section 5.2, i.e. first Test 2.1 and Test 2.5 last, and have two figures each, one for normal and one for FL. Many of the cases made it difficult to estimate the correct velocities, for example, Test 2.4 which was driving off road. One thing to note in a few of the cases with normal tyres is that as soon as the driving settles down a bit, the estimations are back on track. It is, for example, seen at the end of Test 2.1.

Test 2.1 Tight cornering - From Figure 6.13 it can be said that the estimations cannot handle lateral forces well since there are a lot of spikes in the ratios. However, as mentioned previously, when the driving slows down, the estimations are back to performing well. Figure 6.14 shows a similar behaviour, the only difference being that the ratio for FL is lower than the rest, which is where the minispare is located.

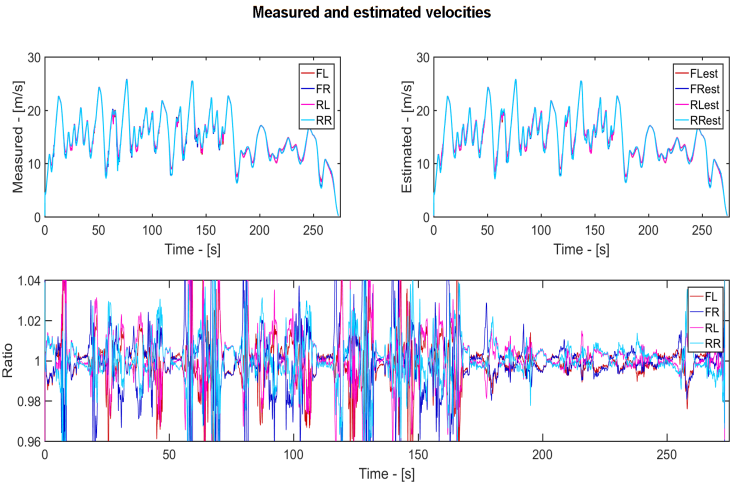

Figure 6.13: Processed data from Test 2.1 with normal tyres

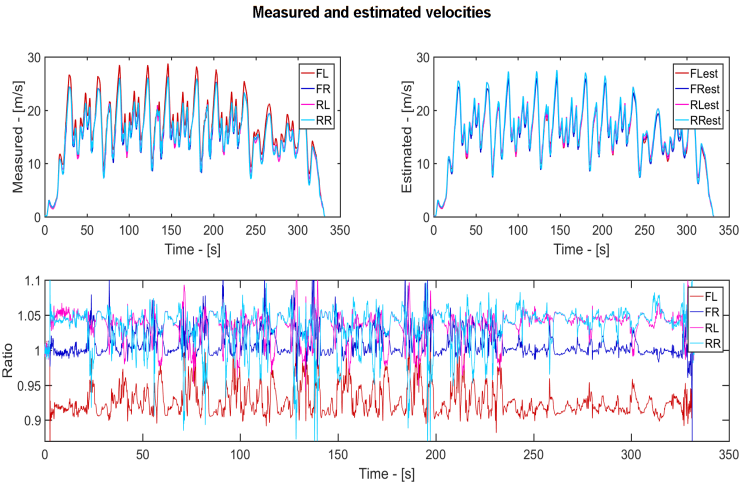

Figure 6.14: Processed data from Test 2.1 with minispare on FL

Test 2.2 High speed - When studying the measured and estimated velocities in Figure 6.15, it seems as though they are quite similar. This can be confirmed by looking at the ratios, however, it also portrays a lot of spikes similar to Test 2.1. The same goes for Figure 6.16 where it is clear that the minispare is located on FL since its ratio is below 0.95.

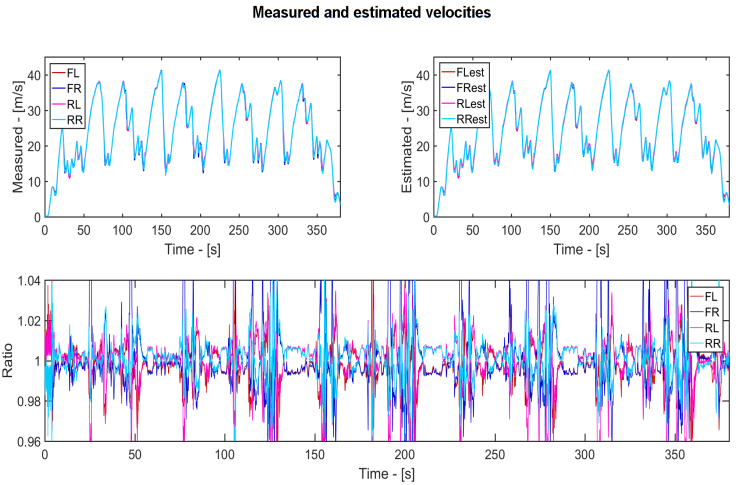

Figure 6.15: Processed data from Test 2.2 with normal tyres

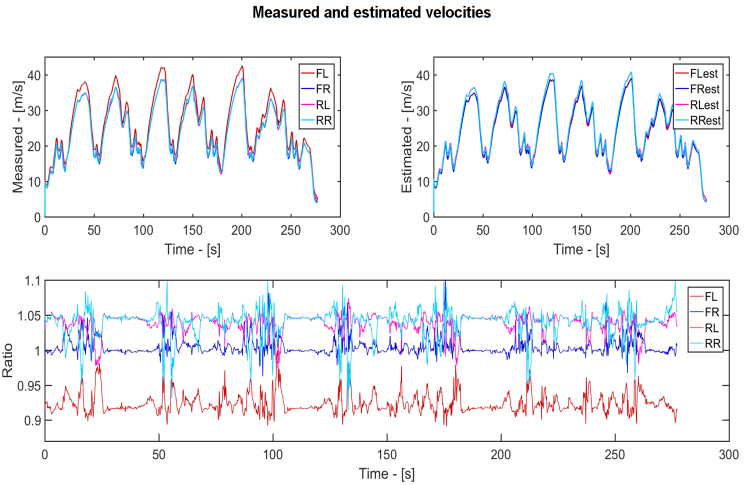

Figure 6.16: Processed data from Test 2.2 with minispare on FL

Test 2.3 Acceleration - The ratio in Figure 6.17 looks quite messy at first glance, however, when noting the scale on the y-axis it can be seen that the ratio is between ± 3 % most of the time. This means that the estimations follow the measured velocities well for accelerations. The estimations perform properly for Figure 6.18 as well and it is clear that FL is the one with a minispare.

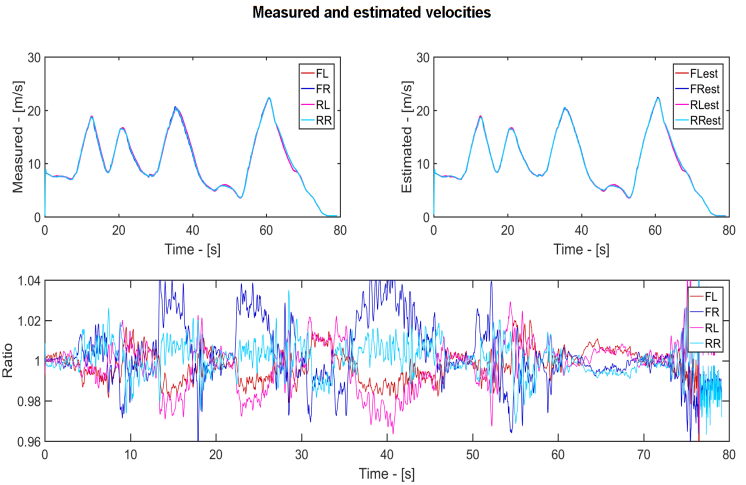

Figure 6.17: Processed data from Test 2.3 with normal tyres

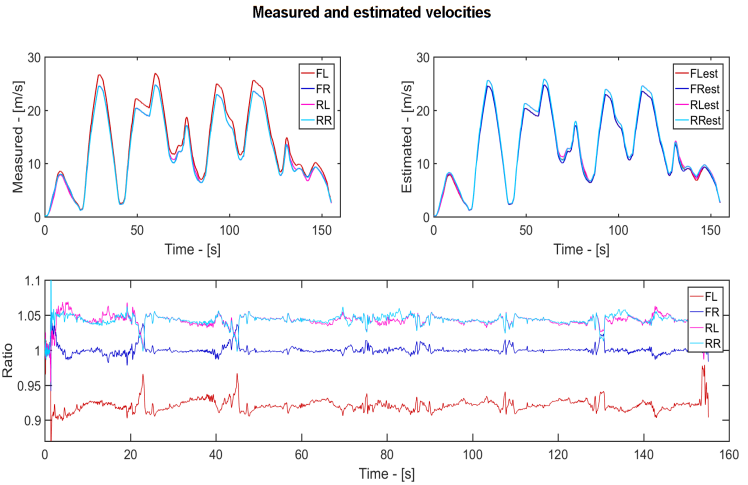

Figure 6.18: Processed data from Test 2.3 with minispare on FL

Test 2.4 Off road - This test is the one that causes the most issues for the estimations. By looking at the ratios in Figure 6.19, it is difficult to come to any conclusions. Even though it is visible in Figure 6.20 that FL is lower compared to the others, it is still challenging to come to a decision. This, since, there are more spikes compared to the other tests.

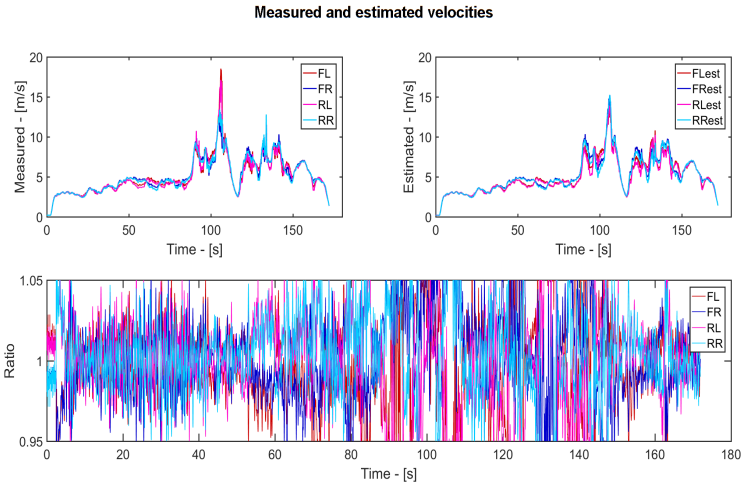

Figure 6.19: Processed data from Test 2.4 with normal tyres

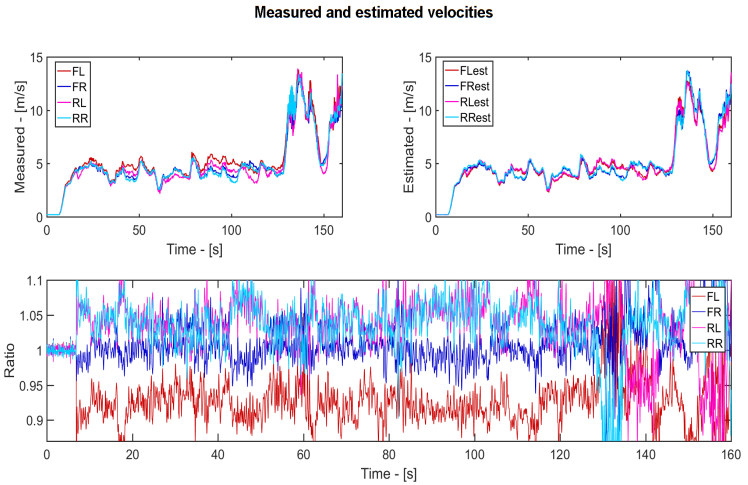

Figure 6.20: Processed data from Test 2.4 with minispare on FL

Test 2.5 Fast turns - In the measured velocity graph for both Figure 6.21 and 6.22, it is possible to see that the tyres behave as stated in Section 2.1 regarding cornering. It is also clear that the estimations perform well when studying the ratios even though they have a few spikes when high longitudinal and lateral forces are generated, similar to Test 2.1. Once again, it is clear that there is a minispare on FL.

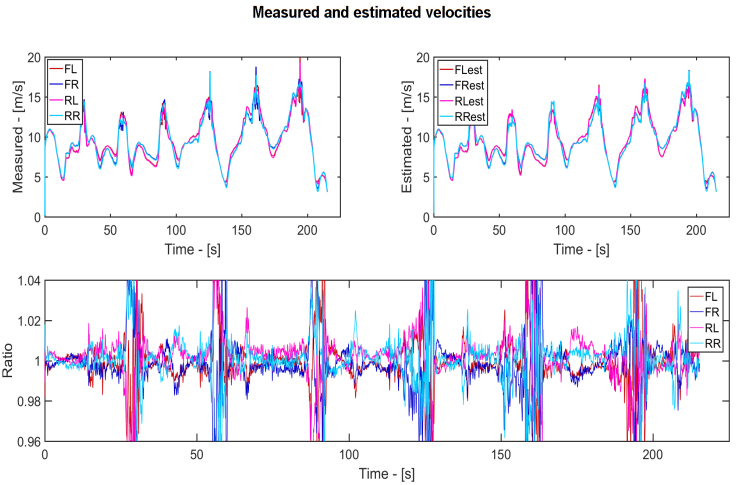

Figure 6.21: Processed data from Test 2.5 with normal tyres

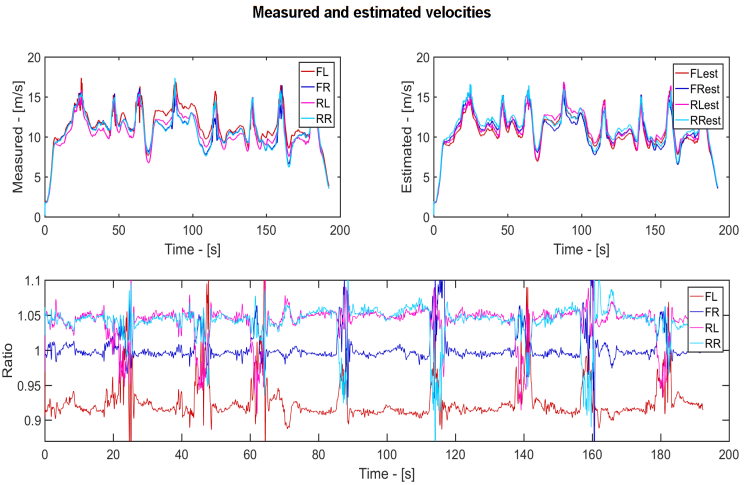

Figure 6.22: Processed data from Test 2.5 with minispare on FL

6.4 Test 2 - Ljungbyhed with Velocity estimation 2

In this section, figures from Test 2.1-2.5 that use Velocity estimation 2 will be shown. As in all the previous tests, only a selected number of figures will be provided in the section and the remaining ratio figures can be found in *Appendix C*. The selection was made with the intent to showcase the difficulties that arise during rough driving in the best way. This was deemed to be the case when a minispare on FL was being used since all the other wheel velocity estimations should be very close to the measured ones, as shown in Section 6.2. That section also proves the predicted patterns in Section 4.3 to be true for both the minispare being placed on front left and rear right, hence, only one of them is necessary for this section.

Each test will be represented by two figures, one showing the measured and estimated velocities during FL minispare usage and one figure illustrating the velocity ratios. The first figure will be divided into four graphs that show all the wheel speeds individually while the second figure shows the standard tyre velocity ratio in the top graph and the minispare velocity ratio in the bottom graph. All ratio plots will be based on estimations from rear left, except for the RL ratio that uses the rear right estimation. This since there is little difference between the two during most of the time and where there is a difference it can be seen in the two front wheel velocity graphs.

As explained in Section 6.3, the ratios will be less smooth due to the estimations not being quite as good during rough driving. It will also be visible that when the driving calms down a bit, as at the end of Test 2.1, the estimations are back to being close to the measured ones.

Test 2.1 Tight cornering - Figure 6.23 illustrates that the measured velocity is higher than the estimated ones for front left. When looking at Figure 6.24 it can be seen that the estimations are not that close until the driving slows down but it is also visible that the FL ratio is continuously lower than the other ones during minispare usage.

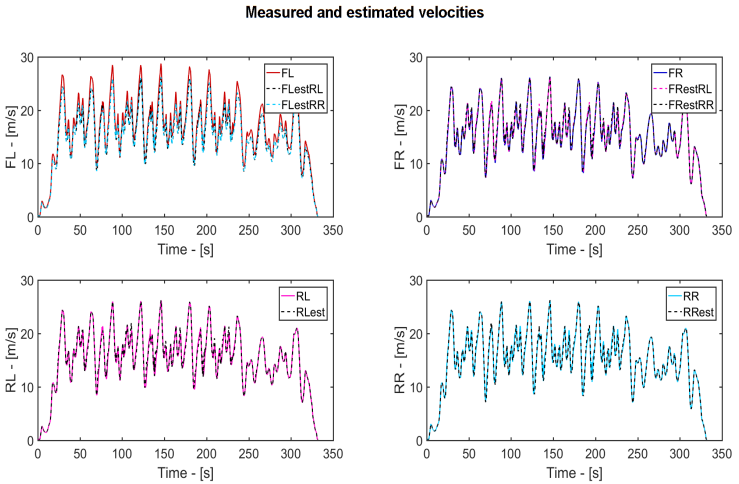

Figure 6.23: Processed data from Test 2.1 with minispare on FL

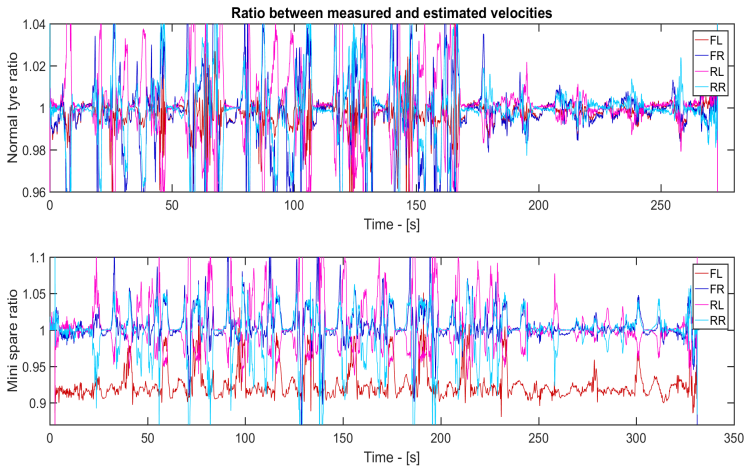

Figure 6.24: Ratio for Test 2.1 for normal tyres and minispare on FL

Test 2.2 High speed - This test includes fewer turns than the previous test and Figure 6.25 together with Figure 6.26 shows that the estimations are good during straight acceleration on asphalt and worse during cornering. Despite this, the minispare ratio follows the pattern that it should.

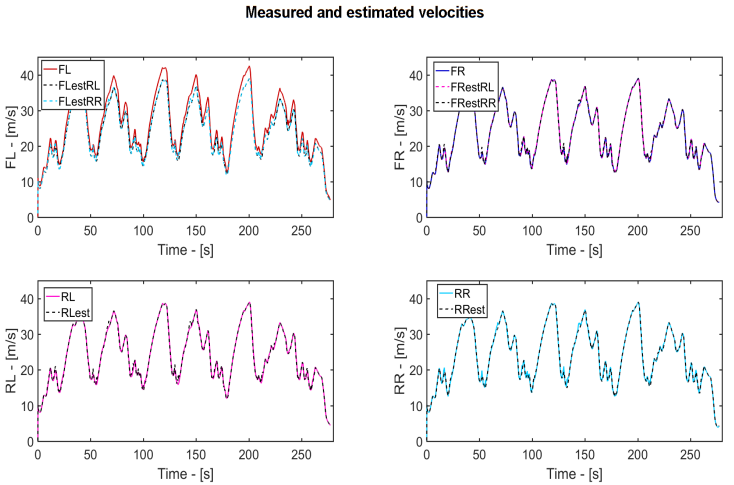

Figure 6.25: Processed data from Test 2.2 with minispare on FL

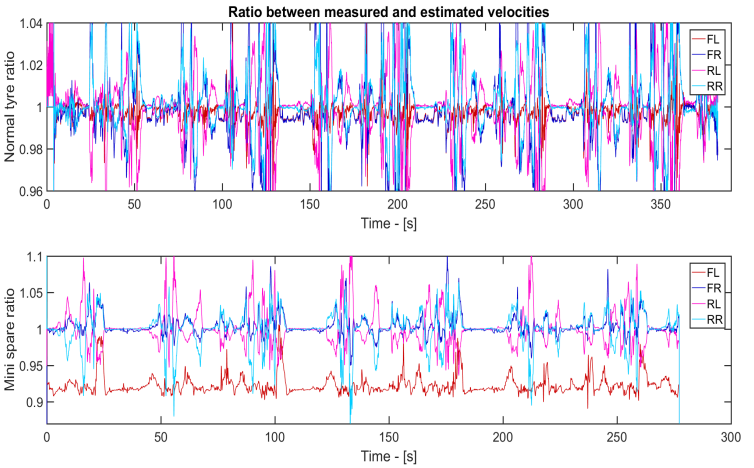

Figure 6.26: Ratio for Test 2.2 for normal tyres and minispare on FL

Test 2.3 Acceleration - Looking at Figure 6.27, all estimations seem to follow the measured velocities well, except for FL where they are too low. This is further proven in Figure 6.28. Even though the normal tyre velocity ratio seems to be messy it is still mainly between $\pm$3-4 %.

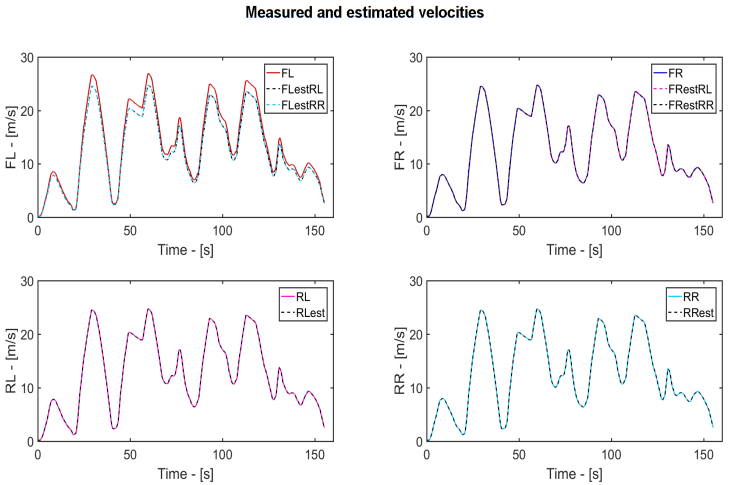

Figure 6.27: Processed data from Test 2.3 with minispare on FL

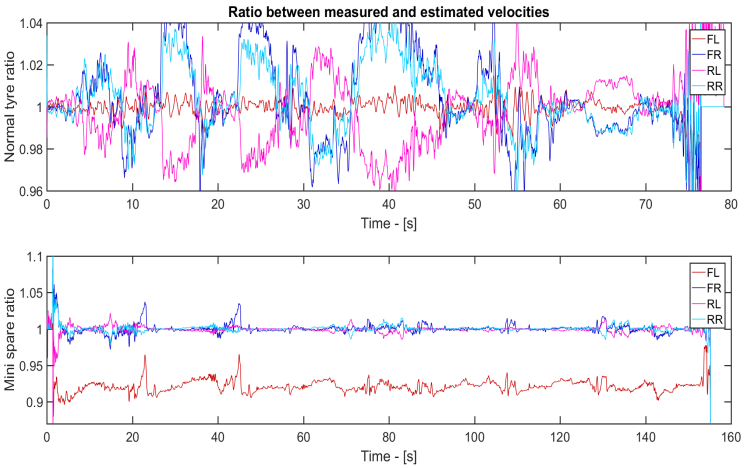

Figure 6.28: Ratio for Test 2.3 for normal tyres and minispare on FL

Test 2.4 Off road - In this test, it can be seen from Figure 6.29 that there is some difference in the estimations depending on if the rear left or rear right velocity is being used. The first ratio in Figure 6.30 shows a greater error span than the previous tests and in the minispare graph, the pattern is still visible, but it is not as stable.

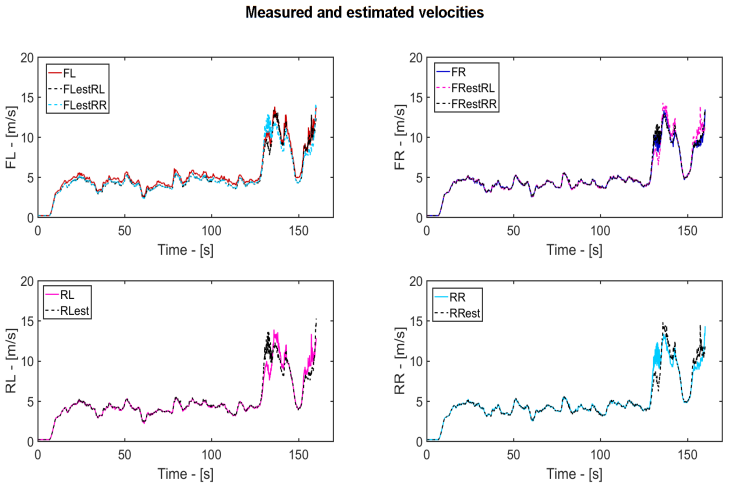

Figure 6.29: Processed data from Test 2.4 with minispare on FL

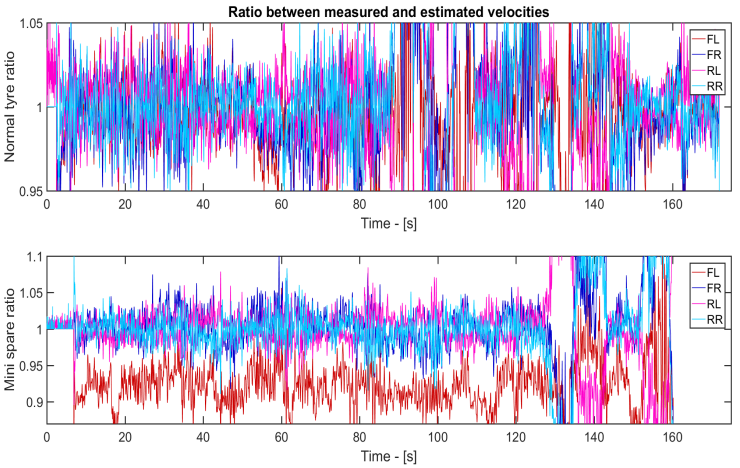

Figure 6.30: Ratio for Test 2.4 for normal tyres and minispare on FL

Test 2.5 Fast turns - Both Figure 6.31 and 6.32 show that the estimations are good although some spikes can be seen in the ratios. These spikes occur when the combination of lateral and longitudinal forces is at its peak and make it difficult to see that the minispare is placed on FL. However, the minispare placement is clearly visible during the entire time otherwise.

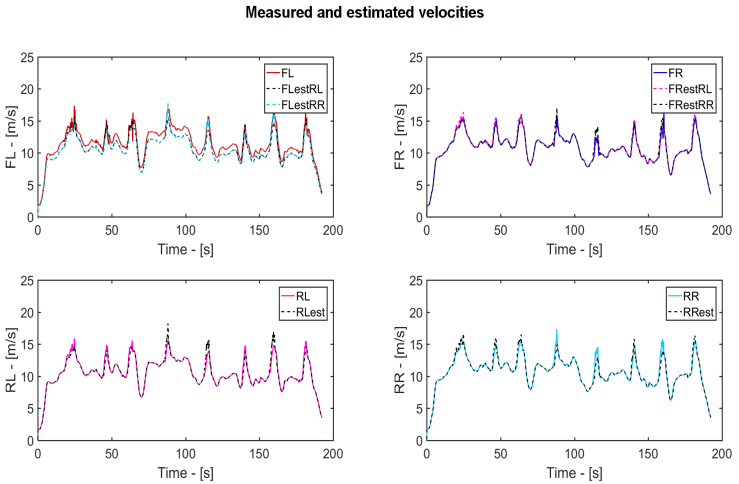

Figure 6.31: Processed data from Test 2.5 with minispare on FL

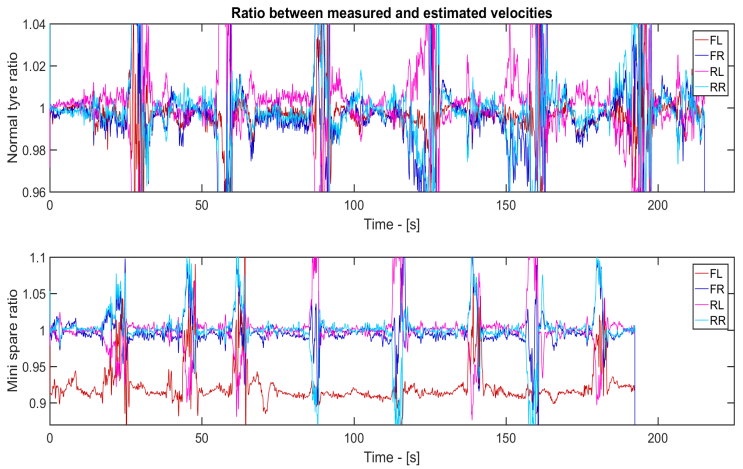

Figure 6.32: Ratio for Test 2.5 for normal tyres and minispare on FL

7

Detection algorithms

After reviewing the results from the previous chapter, it was decided that both velocity estimations performed well enough to use them to detect minispare usage. In most tests, the behaviour of the minispare was so distinct, regardless of estimation, that it could be studied to decide the detection. Therefore, Velocity estimation 1 and 2 were expanded into Detection Algorithm 1 and 2. They included a velocity estimation, a comparison of measured and estimated velocities to detect a minispare, and an estimation of the radius of said minispare.

The two detection algorithms follow the same basic structure that can be seen in Figure 7.1. They start with a velocity estimation, with the help of Velocity estimation 1 and 2 in Chapter 4 and a summation of the estimations for three seconds are then done. This is, to then be able to calculate an average ratio between the estimated and measured velocity during that period. Three seconds was deemed to be a good time period to reduce the impact of the spikes seen in Section 6.3 and 6.4 while not making the algorithms too slow. Both longer and shorter time periods were tested but three seconds gave the best results. The ratio is then compared to some set limits that are different depending on which algorithm it is. These limits where set by looking at the velocity graphs in Chapter 6 and then tuning them until detection performance was satisfactory. From there, a suspect can be set regarding if there is a minispare or not and where it is located. The *suspected normal* and *cannot decide* was added in the final stages of the creation of the algorithms, the reasoning for this is explained in the sections that follow. It is then controlled if the latest five suspected are the same, or the latest six are all the same except for one *cannot decide*, if that is true then detected can be set to the same value as suspected for the rest of the time. If not, the whole procedure starts over without setting a detection. The choice of having five or six suspected was to make the algorithms as safe as possible without compromising the detection time. It will be seen in Chapter 8 that this choice was important in rough driving scenarios. Detected is the variable that decides whether there is a minispare or not, therefore suspected was added as a safety precaution to make sure that the algorithm is sure before making a decision.

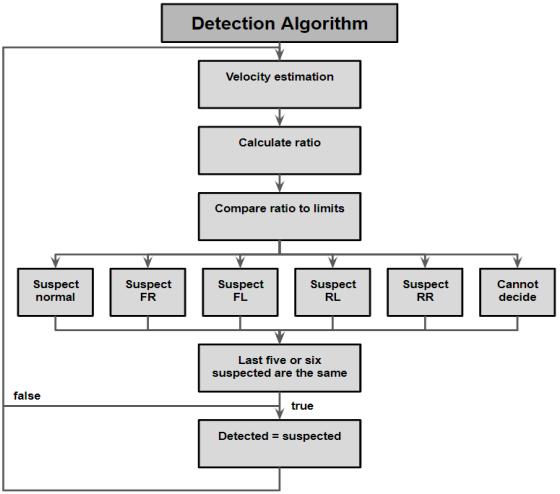

Figure 7.1: Structure of the detection algorithms

To simplify the interpretation of the figures in this chapter, and the rest of the report, different numbers will be assigned to the wheel positions of the car for the suspected and detected graphs. A minispare on FL will be denoted as 1, FR as 2, RL as 3 and RR as 4. While 0 will be representing both *normal* and *cannot decide* until the final step in Figure 7.2 and 7.3. After that, it will only represent *normal* and -1 means *cannot decide*.

7.1 Detection algorithm 1

In the first draft of this algorithm, which is an expansion of Velocity Estimation Algorithm 1, not a lot of safety measures were in place. For a minispare to be suspected, and later detected only the corresponding ratio needed to be lower than a certain limit and the ratio of the other wheel on the same axle needed to be above said limit. The idea was that, since, as seen in Section 6.1, the ratio for the minispare is almost always lower than the rest and below 1, a limit smaller than 1 could be set. It can also be seen in that section that the FR ratio is the only one that is close to 1 when there is a minispare on FL, and thus the ratio for that wheel would have to be larger than the limit. The same logic was used to be able to suspect and detect a minispare on any of the other positions. After using it on the Test 1 data, it seemed to perform well enough. However, after looking at the data from Test 2, the results were not satisfactory as it suspected the wrong wheel too many times and some extra safety measures had to be applied.

The first safety measure to be added was to compare all the ratios before being able to suspect a minispare. This meant that the previous limits were still in place but the ratio for the wheels on the opposite axle needed to be above a limit as well. When trying this on the Test 2 data, minor improvements could be seen but the overall performance was still too poor. After looking at some more parameters from the data, it was discovered that the algorithm sometimes suspected the wrong wheel when the combination of a_x and a_y were too big, meaning that a lot of lateral and longitudinal wheel slip were present. Hence, it was added that if they were too big, the data at that timestamp would be discarded. The last thing to be incorporated was to be able to detect that there was no minispare and to make it clear when no decision could be taken since it was not possible to differentiate between them before. To suspect that all the wheels were standard size, all wheel velocity ratios needed to be within a tight span. If they were not in that span and no minispare could be detected or if the vehicle had been standing still, no decision could be taken. After this expansion, the detection algorithm was giving almost exclusively correct suspected minispare and hence, correct detection and it was decided that the algorithm was completed. During the entire process of enhancing this algorithm, the different limits have been tuned through iterations.
To clarify, the steps that were taken to improve the algorithm were the following:

1. Checking if the minispare ratio is lower than a limit and if the ratio for the other wheel on the same axle is higher than said limit

2. Adding a comparison of all ratios and making sure that they are above the limit

3. Checking if the sum of lateral and longitudinal forces is within a limit

4. Making it clear when there was no minispare or if a decision could not be made

All of the steps and their improvements can be seen in Figure 7.2, where the data is taken from Test 2.1 with a minispare on RL. To make it as difficult as possible for the algorithm, the measured data from the minispare were scaled to make the difference between it and a normal tyre smaller. The change from step 1 to step 2 gave, as stated previously, some minor corrections, mostly that a few of the wrongly suspected minispares were now suspected as 0. The largest improvement, as can be seen in the figure, was in step 3, where all the wrongly suspected minispares disappeared. It also took away some of the correctly suspected minispares, however, since it did not change the detection time, it was deemed to be a safer, and therefore better, option than step 2. In the last step, it can be seen that all of the previously suspected 0 are now -1 which means that in those timestamps a decision could not be made.

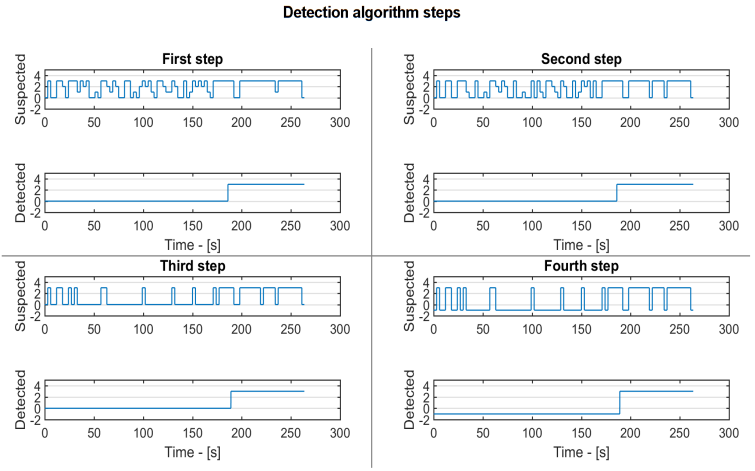

Figure 7.2: Steps for Detection Algorithm 1, using scaled data from Test 2.1 with minispare on RL

7.2 Detection algorithm 2

At the early stages of expanding Velocity estimation 2 into a detection algorithm, only the estimations based on the rear left velocity were used. This meant that the ratios that were available for comparison were FL, FR, and RR. To suspect a minispare on RL, all ratios needed to be above a limit higher than 1. For another wheel to be suspected, the corresponding ratio needed to be below a limit smaller than 1 while the others had to be above that limit. The motivation behind this is the ratio patterns seen in the figures in Section 6.2. As in Detection Algorithm 1, this first step was good enough for Test 1 but not for Test 2. Therefore, some additional features needed to be implemented.

To minimise the amount of wrongly suspected minispares, the estimations based on RR were also used. Because of this, more ratios could be utilised for suspecting a minispare, two for each front wheel and one for each rear wheel. The new ratios were used in the same way as the previously mentioned ones and added to the constraints. For example, a suspected minispare on RL was now obtained by confirming that the RL ratio from RR was below the low limit and the other ratios from RR had to be above that limit in addition to the earlier conditions. After this, the performance was satisfactory with little to none wrongfully suspected minispares with the exception that it was not possible to see the difference between normal tyres and not being able to make a decision. Therefore, a check to suspect and detect normal tyres was implemented by making sure that all ratios were inside a tight span. If none of the conditions for either normal tyres or minispare are true or

if the vehicle has been standing still, a decision could not be made. When all these additions were done, the detection algorithm performed a satisfying result and was deemed to be finished. The additions also included some iterations and alterations regarding the limits.
The steps that were taken to enhance the algorithm were, therefore:

1. Estimation based on only RL and comparing the ratios to a limit
2. An additional estimation based on RR and comparing all ratios to a limit
3. Making it clear when there was no minispare or if a decision could not be made

Figure 7.3 shows the steps that were taken to reach the final algorithm. The data used is from Test 2.1 with a minispare on RL, however, the measured data for the minispare has been scaled to make it more difficult for the algorithm. It is apparent that step 2 makes the detection algorithm more certain since it does not suspect a wrong minispare at any time. Every wrongly suspected minispare, together with a few correctly suspected, is now 0 which improved the safety immensely. The last step moves every 0 down to -1, meaning that no decision could be made, and not that normal tyres were suspected. None of the steps affected the detection time which means that all of them could be used to improve the final algorithm without any consequences.

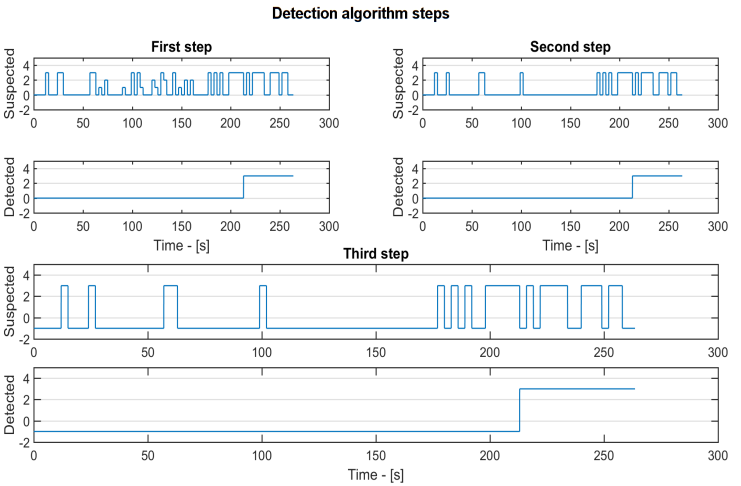

Figure 7.3: Steps for Detection Algorithm 2, using scaled data from Test 2.1 with minispare on RL

7.3 Radius estimation

The reason for estimating the radius is to be able to compensate the systems affected by it in a correct manner. Both detection algorithms follow the same structure when it comes to estimating the radius. In Figure 7.4 it can be seen that, for the radius to get estimated, detected has to be equal to suspected and a minispare has to be present, i.e. suspected > 0. When this is true, a summation of the latest 200 values is done by multiplying each ratio with the original radius set in the car. A radius is then calculated by taking the mean value of this sum and saved in a vector. If the latest three radii in that vector are within a relatively large span, an approximated radius is set. It is then checked if the last four approximated radii are within a smaller span, if that is the case, a decided radius is set. Note that both the approximated radius and the decided radius are variables used to send information to the vehicle.

In the early stages of the estimation, the decided radius was set directly by the calculated radius, from the second step in Figure 7.4, meaning that the approximated step was not done in between. The reason for adding the approximated radius was that, since the decided span was small, it took too long to set a new radius without it. It was decided that it was more beneficial to set a rough estimation as soon as possible, this to reduce the radius error for the minispare and hence, minimise the effects of having a wrong value. When this new value has been set, the smaller span can be used to decide a more accurate radius.

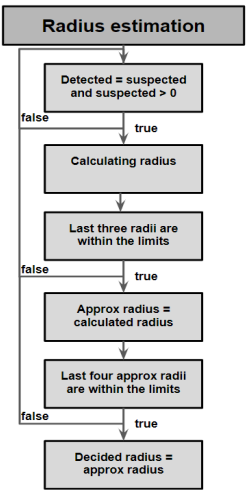

Figure 7.4: The structure of the radius estimation

There are only a few differences between the detection algorithms when it comes to the radius, one being that they use different velocity estimations. Another is that Algorithm 2 uses a mean value of both the ratios with estimations from RL and RR to calculate the radius for the front wheels. Algorithm 1 only has one estimation to make use of, hence the difference.

In Figure 7.5, the estimations for both algorithms are shown with the data from Test 1 part 1 and a minispare on FL. There is not a lot of difference between the two, which is reasonable since they use the same structure. The starting value of the blue line represents the standard wheel size and when it returns to this value it means that a radius could not be set. When comparing the approximated radius to the decided, the decided does not always give a more accurate result, even though it is more stable around the correct radius.

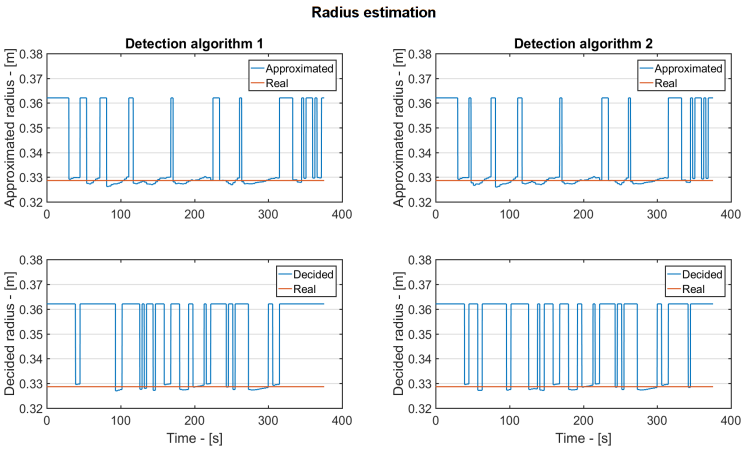

Figure 7.5: Radius estimation for Test 1 part 1 with minispare on FL for both detection algorithms

Since this was an additional task for the thesis if time admitted, it was not a priority to improve the method. Therefore, there will not be any additional figures on this matter in the main text, instead, they can be found in *Appendix E*.

8

Results from detection algorithms

To validate the expanded algorithms, described in the previous chapter, figures illustrating when a minispare, or lack thereof, would have been suspected and detected will be provided. They will show the results from the same tests as in chapter 6, meaning that data from Test 1 part 1, 3, and 5 and Test 2.1-2.5 will be used. With the help of these figures, the two algorithms can be analysed individually and later compared to each other.

Each section in this chapter will provide the results from one test using one of the algorithms as well as a description of the behaviour. Since not all test cases will be shown, the rest of the results are shown in table form in *Appendix B* for Test 1 and *Appendix C* for Test 2.

There are some important factors to consider when reading this chapter. The first one being that the period that each part of each test has been conducted is different. Therefore, it might seem like some detection times are very long, when the reality is that the time shown is much shorter and the detection time might be similar or even faster than the others. Another important factor is that each figure will show the result of when a minispare has been used and when all tyres have been of normal size. Lastly, there will be no scaling of the measured wheel velocities as in chapter 7 to get as accurate results as possible.

8.1 Test 1 - City drive with algorithm 1

In this section, the performance of Detection Algorithm 1, during some parts of Test 1, will be presented in Figure 8.1. The parts that will be discussed are equal to the ones in section 6.1, meaning part 1, 3 and 5, and is chosen for the reasons stated there. It is also the same minispare position, FL, as previously to easily be able to analyse the velocity estimations together with this figure. The bottom right graph in the figure shows part 5 for normal tyres, this is to illustrate that the algorithm can detect 0 in the most difficult scenario from Test 1.

Both part 1 and 3 are handled well by the algorithm, no wrongly suspected minispares are done and it is only a few times when a decision cannot be made. This does not affect the detection since when a -1 is suspected and the closest five suspected are all 1, the six latest suspected only includes one -1 and a detected can still be set. The detection time for part 1 and 3 are both in the range of 20-30 seconds, which can be considered as a good result, this will be discussed more in chapter 9. In part 5 for both normal tyres and minispare, the beginning includes reversing for a little while and then standing still while changing gear before being able to drive forward. This can be seen in both graphs as the little suspected tyre at the beginning followed by a short period of -1. Therefore, the detection time is a bit longer than that for part 1 and 3, however, it is still below 50 seconds. For a fair comparison, the first part that includes the reversing should be ignored and the time would start when the car starts moving forward.

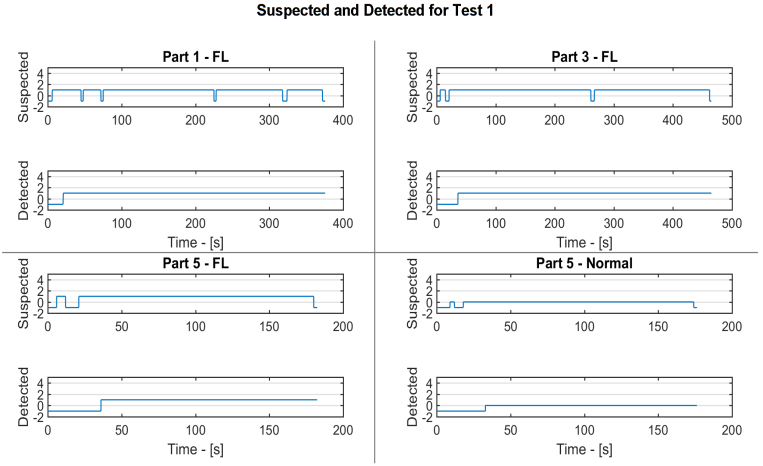

Figure 8.1: Suspected and Detected for different parts of Test 1, one with normal tyres and the rest with minispare on FL

8.2 Test 1 - City drive with algorithm 2

Figure 8.2 illustrates how Detection Algorithm 2 performs with the data from Test 1, where part 1 is with minispare on FL, part 3 and 5 with minispare on RL, and normal tyres for part 5. The reasoning behind the choice of cases is the same as in section 6.2 as well as simplify the analysing of the velocity estimations to the detection.To not only show cases of the minispare being placed on FL, as for Algorithm 1, is because it is interesting to see the results when the minispare is placed on one of the wheels used in the estimations.

When looking at part 1 in the figure, it is clear that the case is dealt with sufficiently. The algorithm suspects a -1 in the end, the cause for this is that the car is standing still at that point. In part 3, the behaviour is quite similar except for a suspected 3 followed by a short period with -1 in the beginning. This is because of reversing and then standing still to change the gear before being able to drive forward. The detection time is affected a little by this since it cannot be set directly, however, it is still acceptable. Both graphs showing part 5 indicate that the algorithm can handle driving slow in a parking lot without any struggle. Only two -1 are suspected when normal tyres are being used which is due to standing still.

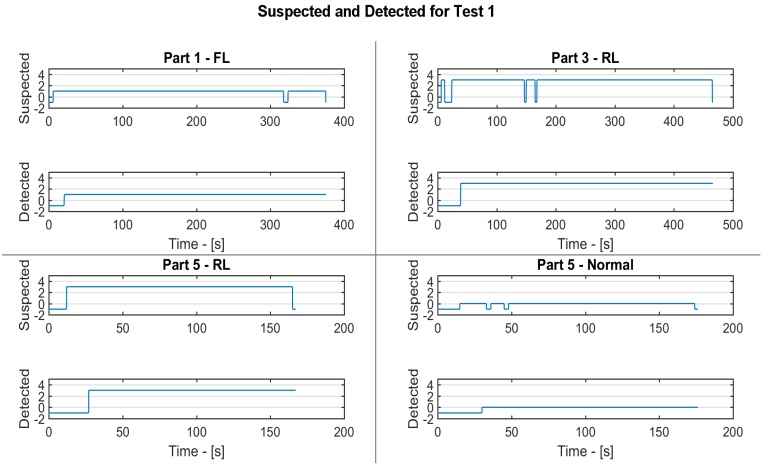

Figure 8.2: Suspected and Detected for different parts of Test 1, one with normal tyres, one with minispare on FL and two with minispare on RL

8.3 Test 2 - Ljungbyhed with algorithm 1

Figures showing the results from Test 2.1 to 2.5, using Algorithm 1, will be shown in this section. Each one will include plots from when a minispare was placed on FL and the corresponding test when no minispare was present. The reason for presenting them this way is to be able to discuss the performance in a manner that is as cohesive as possible.

It can be seen, in Figure 8.3, that the suspected parts include a lot of -1 which is expected since the driving was very aggressive. However, it implies a good performance since there are no wrongfully suspected wheels, and the detection times are short, all under 50 seconds. There is also a time point in *Test 2.1 - Normal* when detected changes to -1 before it goes back to 0 again. This behaviour can be seen in several figures in this and the following section and will be explained in chapter 9.

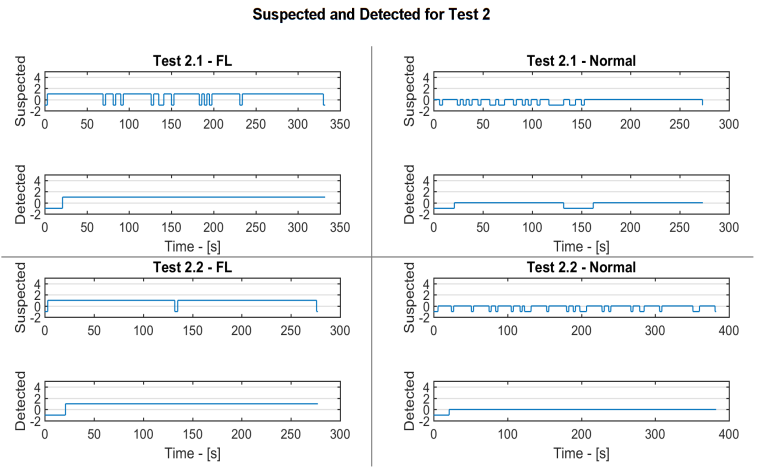

Figure 8.3: Suspected and Detected for Test 2.1 and 2.2 with minispare on FL and normal tyres

An example of when it is important to look at the different time axes is seen in Test 2.3 in Figure 8.4. The algorithm seems to be much slower at detecting that normal tyres are being used than a minispare and even though there is a difference, it is not that big when looking at the detection time. For off road driving, there is a lot of incorrectly suspected wheels in the normal tyres case. This demonstrates the importance of needing suspected to be the same value a number of times before a detection decision can be taken.

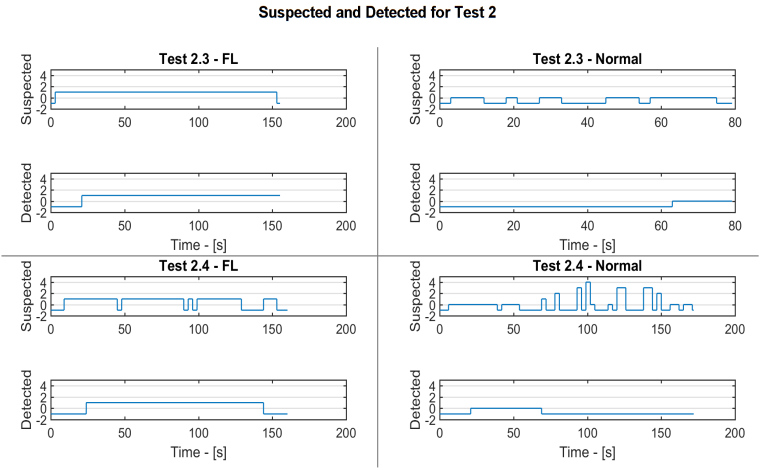

Figure 8.4: Suspected and Detected for Test 2.3 and 2.4 with minispare on FL and normal tyres

There is no major problem with Test 2.5 as seen in Figure 8.5. The detection times are both around 25 seconds and the single wrongfully suspected minispare is not an issue because of the structure of Algorithm 1.

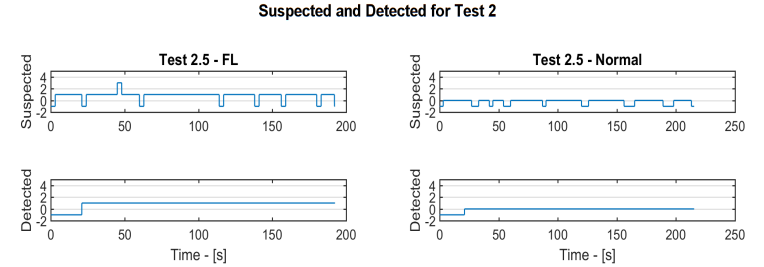

Figure 8.5: Suspected and Detected for Test 2.5 with minispare on FL and normal tyres

8.4 Test 2 - Ljungbyhed with algorithm 2

This section will provide the results of using the test data from Test 2.1-2.5 with Algorithm 2 and an analysis of the outcome. Figure 8.6, 8.7, and 8.8 illustrate the same test cases as in the previous section, this is to easily be able to compare and the two algorithms and discuss their results.

Figure 8.6 shows an overall satisfying outcome since there are no wrongly suspected tyres and the detection time is below 50 seconds for all cases except Test 2.1 with normal tyres. In that case, the detection is lost a few times, this is the same behaviour as for Algorithm 1 and will be discussed in chapter 9 as stated in section 8.3. There is a lot of suspected -1 in all cases which were anticipated due to the rough driving throughout the entire test.

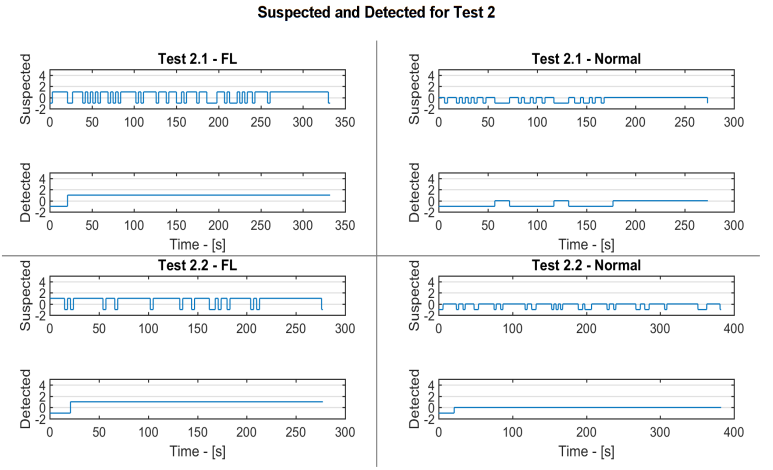

Figure 8.6: Suspected and Detected for Test 2.1 and 2.2 with minispare on FL and normal tyres

For Test 2.3 and 2.4 in Figure 8.7, the behaviour looks good considering the detection time for all cases. When comparing the results, it is clear that the case with normal tyres is worse for both tests. They are less stable than for FL, this is especially true for Test 2.4 where some wrongly suspected tyres can be seen. In that case, it is apparent that *Suspected* is needed to not set *Detected* to a wrong tyre, this will be discussed more in chapter 9. The reason why it is more difficult for the algorithm to decide normal tyres is also explained in that chapter.

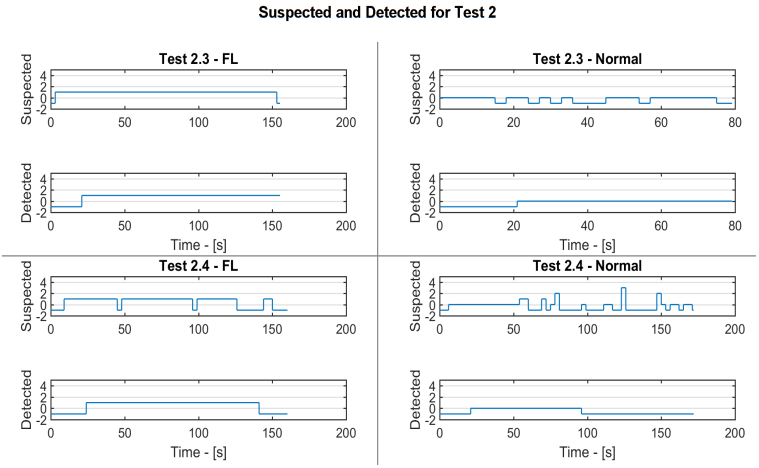

Figure 8.7: Suspected and Detected for Test 2.3 and 2.4 with minispare on FL and normal tyres

Algorithm 2 handles the data from Test 2.5, regardless of minispare or normal tyres, well as can be seen by the steady results in Figure 8.8. There are some suspected -1 in both cases, however, this does not affect the time of detection since the algorithm allows a -1 in the last six suspected tyres if the rest are the same tyre.

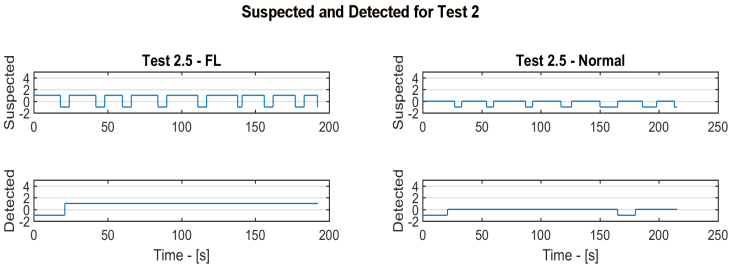

Figure 8.8: Suspected and Detected for Test 2.5 with minispare on FL and normal tyres

9

Discussion and conclusion

This chapter focuses on discussing the results of the thesis as well as concluding the work. It will evaluate certain points that have been commented on in previous chapters and provide possible explanations to them.

9.1 Evaluation of difficult driving scenarios

The driving scenarios from Section 1.2, and the tests investigating them, are listed below.

- low and mid speed cornering manoeuvring - Test 1 part 5 and Test 2.5,
- actual drive torque induced wheel slip - Test 2,
- high front/rear speed differences during acc. and braking - Test 2.1 and 2.2.

All of them caused issues in the early stages of creating the algorithms, however, the first scenario was taken care of easily by tuning the limits in the first step of each method. The other two proved to be a bit more difficult. For Algorithm 1, the restriction on the combination of a_x and a_y was needed to handle them correctly. To take care of them in Algorithm 2, the addition of looking at the ratios based on the rear right estimations, and not only the rear left estimations, was necessary. Before adding the final step for both algorithms, which made it clear when there was no minispare or if a decision could not be made, it was a bit difficult to interpret some of the data. When the step was added, it made it clear that a decision could not be made sometimes for these tests. It also showed that in the cases when a decision could be made, the two steps mentioned above proved to be enough to take care of the difficult driving scenarios.

9.2 The vehicles radius

In Chapter 4 it is described that the velocity ratio of the minispare should be equal to the ratio between minispare and normal tyre radii. This might be confusing when looking at the ratio plots since they show a difference closer to 9 % than 8.4 %. The reason for this is that the car uses a set value for the radius that, in this case, is larger than the wheels used. Therefore, the wheel speeds are seen as faster than reality resulting in a bigger velocity difference. However, since the velocity estimations use them, the ratios are correct in regard to the set radius and should still provide an accurate result. The detection algorithm should, therefore, work regardless of wear and tear.

9.3 Test 3 with Volvo XC40

As stated in Chapter 5 the figures from Test 3 can be found in *Appendix D*. In the figures, it can be seen that a minispare that is 5.3 % smaller than the original size can be detected without any difficulty. These results are important because the smaller the difference between them is, the harder it gets for both algorithms to detect a minispare since they might misinterpret it as a normal sized tyre. Any minispare that is closer to the standard size will be too difficult to detect with these methods.

9.4 Radius estimation

It is clear from the results of the radius algorithm, both in Section 7.3 and *Appendix E*, that there is room for improvement. A possible explanation for the lack of performance is that the velocity estimations can deviate ± 2 %. Since these are used for the calculations, the same margin of error applies to the radius. For the detection algorithms, this deviation is accounted for in the different limits. However, the radius is used as an input for many systems in a vehicle, therefore it needs to be more precise. Because of this, there may be a need to look at other factors but as mentioned in Section 7.3 this was not the main focus and, hence, no attempts were made on improving the method.

9.5 Importance of suspected variable

In parts of Chapter 8, it is stated that *Suspected* is important to not make any mistakes in *Detected*. The condition for setting detected is that the five latest suspected values need to be equal or that out of six values, five are the same and one is -1. The -1 means that the data cannot be interpreted as a recognisable pattern, while other values imply that a decision can be made. Therefore, one -1 is acceptable but anything other than that makes the data too indecisive to set detected. The reason behind the number of equally suspected tires needed in a row is to prevent detecting a tyre when the data is as unsteady as in Test 2.4. With data like that, the algorithms struggle since the velocity estimations are based on a steady state, which is far from the case when driving off road as well as the rest of Test 2.

9.6 Difficulties with Test 2 - Ljungbyhed

To challenge the algorithms with driving scenarios that included a lot of driver induced wheel slip and other difficult factors, Test 2 was performed. The rough driving made it difficult to decide a suspected at some times, which can be seen in Table C.1-C.6 in *Appendix C*. It was also challenging to replicate each test case in an exact manner. For example, Test 2.1 with a minispare of FL is not identical to when normal tyres on all positions were used regarding the velocity, wheel slip, etc. This might be a reason why there is a difference in the result pattern between normal and FL, shown in the figures in sections 8.3 and 8.4. The fact that normal is less steady than FL could also be because of the way the limits for suspecting a tyre are set which are more restrictive for the all normal tyres case. It was decided to have tighter limits for the normal tyre case, to be able to detect a minispare that deviates, in size, as little as possible. For normal driving conditions, as shown in the results for Test 1, these limits are not an issue when it comes to the detection verdict.

9.7 Detection time

To consider a detection time as good, the driving scenario has to be taken into account. For example, it is acceptable with a longer detection time for the driving at Ljungbyhed compared to city driving. However, it should not be any longer than 60 seconds in general to, with certainty, perform better than the current method that BorgWarner uses. Both algorithms described in this report, usually manage to detect a minispare within this time frame, even in adverse driving conditions, see *Appendix B-D*.

9.8 Comparison of detection algorithms

There are two main differences between the derived algorithms: One - that they use different velocity estimations; Two - how restrictive they are. Algorithm 1 has a regulation on the sum of a_x and a_y which is not needed for the other algorithm. The reason for adding this condition is explained in Section 7.1 and the impact on the results is clearly positive when studying Figure 7.2. Why this is not needed for Algorithm 2 is most likely due to there being more estimations to make use of. More estimation means more ratios that need to be within certain limits to set suspected which makes the algorithm more restrictive. Therefore, the problems that caused the addition in Algorithm 1 are already taken care of.

Even though these differences exist, they still have the same structure and perform similarly. This is shown in the results presented in Chapter 8, where they are very alike except for *Test 2.4 - Normal*. In this test, both of them suspect that there is a minispare present multiple times, but Algorithm 2 has the lesser amount. As mentioned previously, Algorithm 1 is limited by a_x and a_y, however, they are not big enough during this off road driving to trigger the restriction. The performance difference is, therefore, explained by the fact that more estimations and ratios are used to suspect a minispare in Algorithm 2 as mentioned above.

The method that BorgWarner uses currently has a main objective to precisely determine axle speed difference due to differently sized tyres, and is more complicated in the way that the detection functions in contrast to both algorithms created in this thesis. It is also more selective in what driving scenarios that it can be used in, meaning that the thesis methods can be used in more drive cases, and enable earlier mitigation actions in the all wheel drive, AWD, control strategy. These are the main reasons for being able to reduce the detection time compared to the current method.

9.9 Improvements

The biggest improvement would be to enhance the radius estimation, this has already been elaborated on in Section 9.2 and will therefore not be discussed any further. Another improvement that could be done, even though the results are satisfactory, is to tune the velocity estimations and limits even more.

One thing that has not been mentioned in the report is that when implementing the solution provided, a new condition should be added. This is that when the vehicle has been standing still for a certain amount of time, a wheel could have been changed to or back from a minispare. The detection process should then start over. To implement the algorithms in a car, they would have to be converted to C code.

When doing that, it should be considered unnecessary to perform wheel speed measurements while the vehicle is standing still and, hence, perform any calculations. It would, therefore, be a smarter solution than the current one.

There is an issue of *Detected* changing from a detected minispare to -1, as noted in Chapter 8, meaning that the data cannot be interpreted as any recognisable pattern. However, it would not be a problem in the implementation. This is because when the detected verdict has been set, it should not be able to change until the car has been standing still for a long enough period. The reason for being able to change it in the figures was simply an illustration choice.

9.10 Conclusion

At the beginning of the thesis, a problem formulation was described which stated the main goal, reducing the detection time, and difficult driving scenarios that would be investigated. The main goal has been achieved, for both algorithms, with the help of the results and discussions. From Test 3, the algorithms have been confirmed to not only perform well with a minispare that is 8.4 % smaller but also with one where the difference is only 5.3 %. Therefore, the smallest size difference that can, with certainty, be detected is 5.3 % which is good since the standard deviation for a minispare lies between 5 % and 20 % [8].

There is not much difference when it comes to the performance between the two algorithms and both of them could be implemented for detection purposes. However, Algorithm 2 is the safer choice as demonstrated by fewer wrongly suspected minispares in Test 2.4 when normal tyres were used. When it comes to radius estimation, there needs to be more work done before implementation.

Overall, the thesis work has been successful and it is up to BorgWarner to choose if an implementation should be done and which algorithm to select in that case.

Bibliography

[1] G. Zhang, Z. Yu, and J. Wang. *Mechanical Systems and Signal Processing*. Ohio State University, 2017.

[2] M. W. Sayers. *Vehicle Offtracking Models*. University of Michigan, 1986.

[3] M. Blundell and D. Harty. *The Multibody systems Approach to Vehicle Dynamics*. 2nd ed. Elsevier Ltd., 2015.

[4] R. Rajamani. *Vehicle Dynamics and Control*. Springer, 2006.

[5] H. B. Pacejka. *Tire and Vehicle Dynamics*. 2nd ed. SAE, 2006.

[6] D. Schramm, M. Hiller, and R. Bardini. *Vehicle Dynamics: Modeling and Simulation*. Springer Berlin Hidelberg, 2014.

[7] P. Petterson. *Estimation of Vehicle Lateral Velocity*. Lund University, 2008.

[8] B. Ye, M. Schneider, S. Eswara, M. Tuhro, and V. Luomaranta. “Quick mini-spare detection”. US 9,718,474 B2, Aug. 1, 2017.

A

Map of Landskrona

A.1 Route of Test 1

Figure A.1 shows a map of Landskrona where the route of Test 1 is drawn.

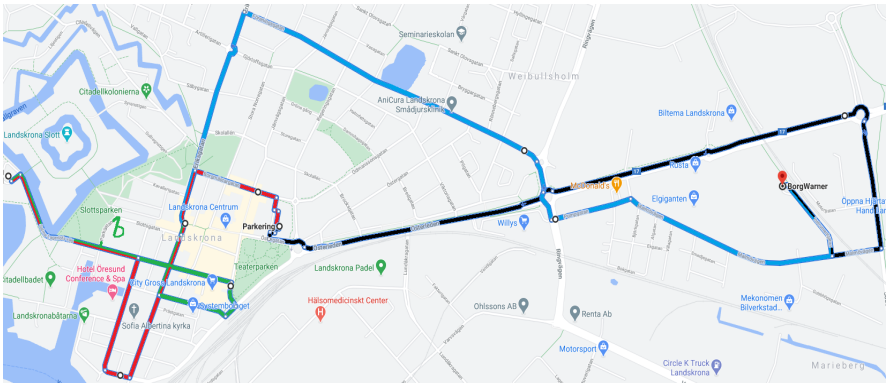

Figure A.1: The black distance is part 1, red is part 2, green is part 3 and blue is part 4. The last part, part 5, was done in BorgWarners parking lot

B

Test 1 - City drive

B.1 Algorithm 1

This section will provide the figures of the velocity estimation and ratios for part 2 and 4 in Test 1 using Algorithm 1, see Figure B.1-B.4. It will also show the ratios for the remaining placements on the minispares in Figure B.5-B.9 as well as a condensed version of the results from *Suspected* and *Detected* in Table B.1-B.5. Note that the mean value of the FL and FR velocities is used for estimating the rear wheel speeds and the mean value of the rear velocities for the front speeds.

Velocity estimations and ratios for part 2 and 4 with normal tyres and minispare on front left

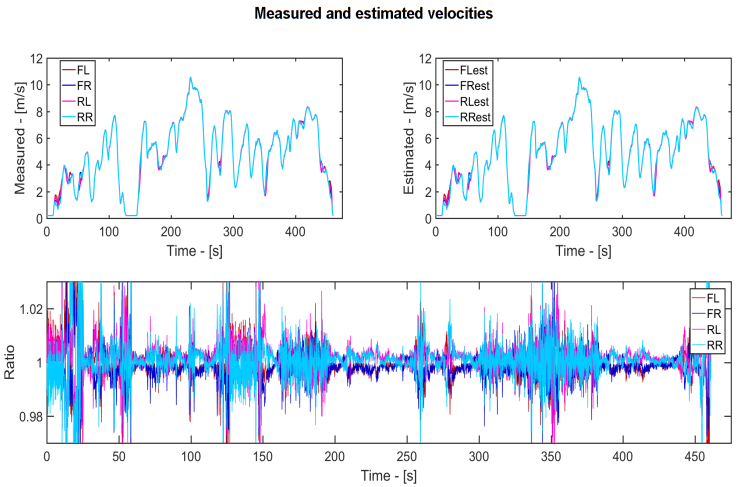

Figure B.1: Processed data from part 2 of Test 1 with normal tyres

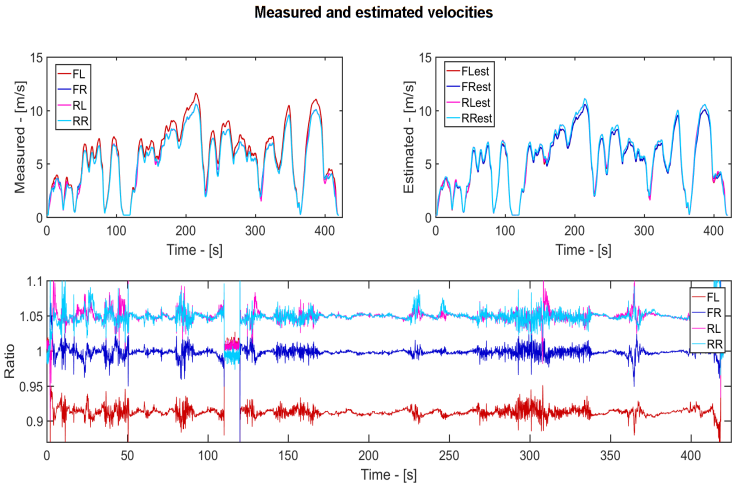

Figure B.2: Processed data from part 2 of Test 1 with minispare on FL

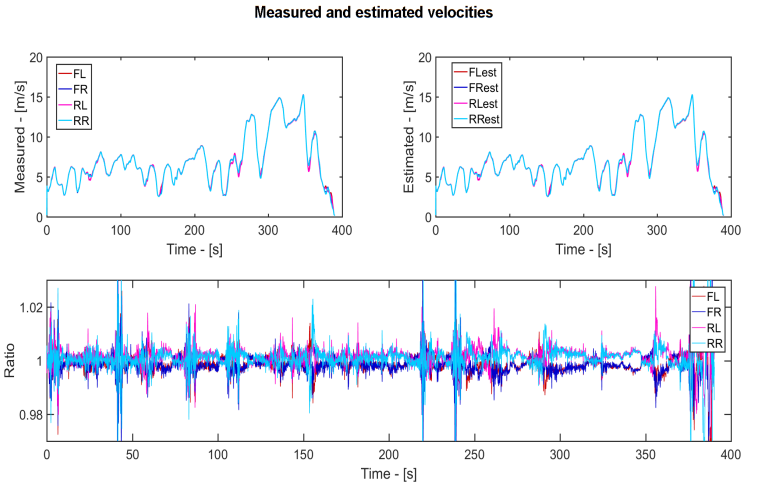

Figure B.3: Processed data from part 4 of Test 1 with normal tyres

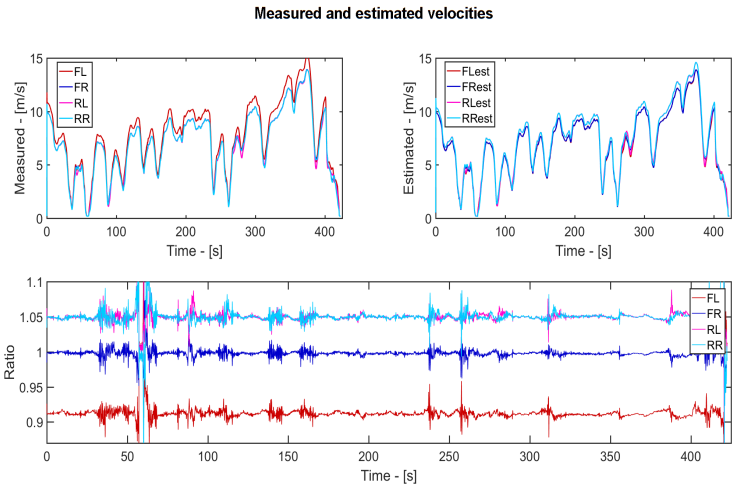

Figure B.4: Processed data from part 4 of Test 1 with minispare on FL

Ratios for part 1-5 with minispare on front right, rear left, and rear right

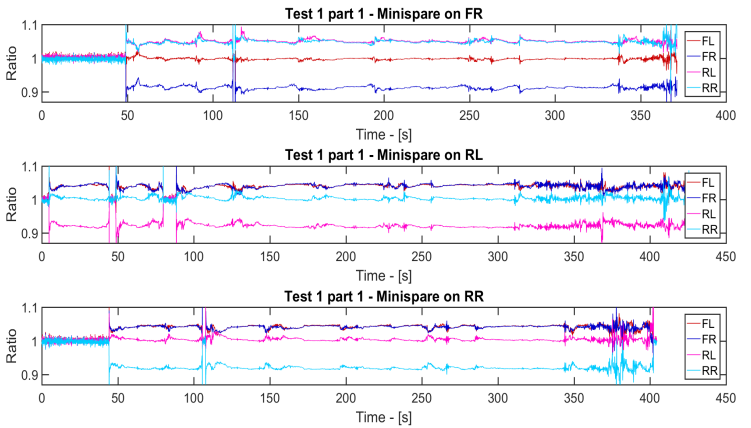

Figure B.5: Ratio for part 1 with minispare on FR, RL, and RR

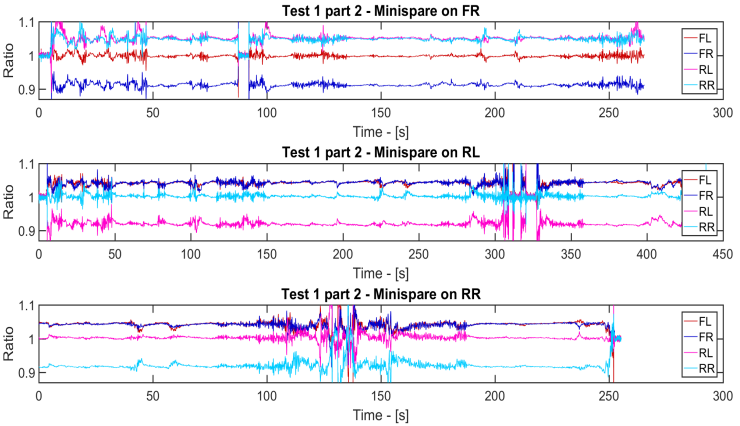

Figure B.6: Ratio for part 2 with minispare on FR, RL, and RR

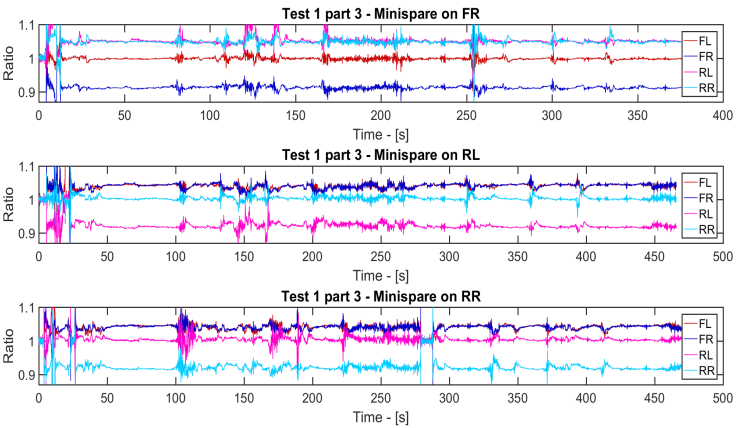

Figure B.7: Ratio for part 3 with minispare on FR, RL, and RR

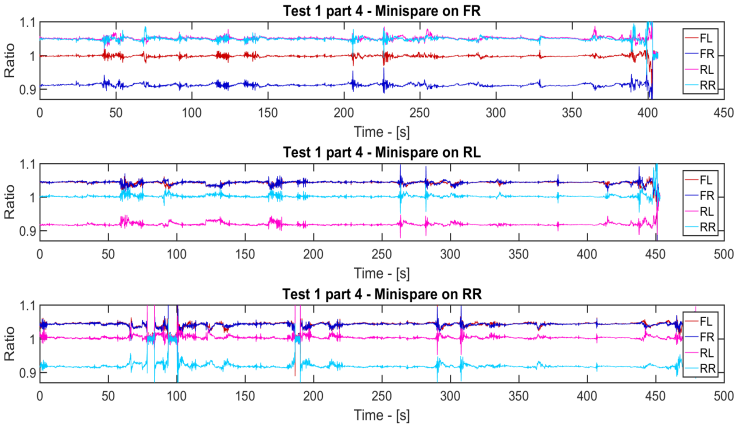

Figure B.8: Ratio for part 4 with minispare on FR, RL, and RR

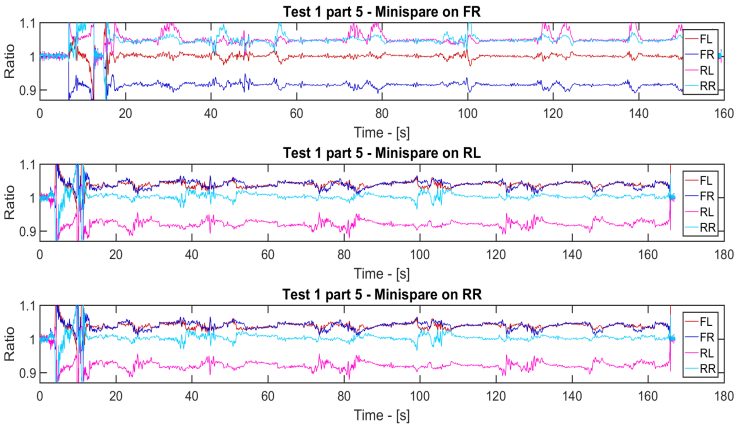

Figure B.9: Ratio for part 5 with minispare on FR, RL, and RR

Suspected and *Detected* for part 1-5

The *Suspected* and *Detected* are shown in table form, even the ones already presented in figures in chapter 8. They will provide the detection time, the number of times *Suspected* set to -1 and the number of times a wrong minispare was suspected. In these tables, Table B.1-B.5, all of the *Cannot decide* are the results from the vehicle standing still.

Part	Detection time	Nr. cannot decide	Nr. wrong suspected
1	25	8	0
2	20	8	0
3	40	5	1
4	20	1	0
5	45	3	0

Table B.1: Result from *Suspected* and *Detected* with normal tyres

Part	Detection time	Nr. cannot decide	Nr. wrong suspected
1	20	6	0
2	20	7	0
3	30	3	0
4	20	3	0
5	45	3	0

Table B.2: Result from *Suspected* and *Detected* with minispare on FL

Part	Detection time	Nr. cannot decide	Nr. wrong suspected
1	75	0	0
2	20	2	0
3	25	2	0
4	20	0	0
5	30	2	0

Table B.3: Result from *Suspected* and *Detected* with minispare on FR

Part	Detection time	Nr. cannot decide	Nr. wrong suspected
1	70	0	0
2	20	3	0
3	35	3	0
4	20	0	0
5	30	2	0

Table B.4: Result from *Suspected* and *Detected* with minispare on RL

Part	Detection time	Nr. cannot decide	Nr. wrong suspected
1	60	0	0
2	25	5	0
3	30	6	0
4	20	4	0
5	25	0	0

Table B.5: Result from *Suspected* and *Detected* with minispare on RR

B.2 Algorithm 2

The figures in this section shows all the ratios that were not shown in the report in Figure B.10-B.16 and a condensed version of the results from *Suspected* and *Detected* in Table B.6-B.10 as well. Note that the ratios shown are all from estimations based on RL except for the RL ratio that uses the RR estimation.

Ratios for with normal tyres, minispare on front left, front right, rear left, and rear right

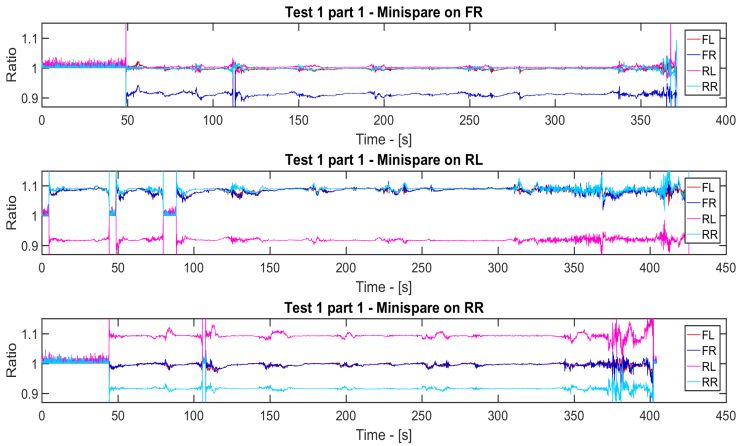

Figure B.10: Ratio for Test 1 during part 1 with minispare on FR, RL, and RR

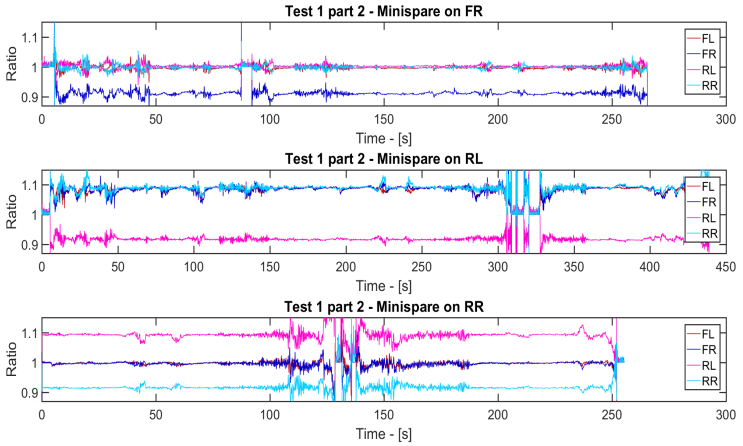

Figure B.11: Ratio for Test 1 during part 2 with minispare on FR, RL, and RR

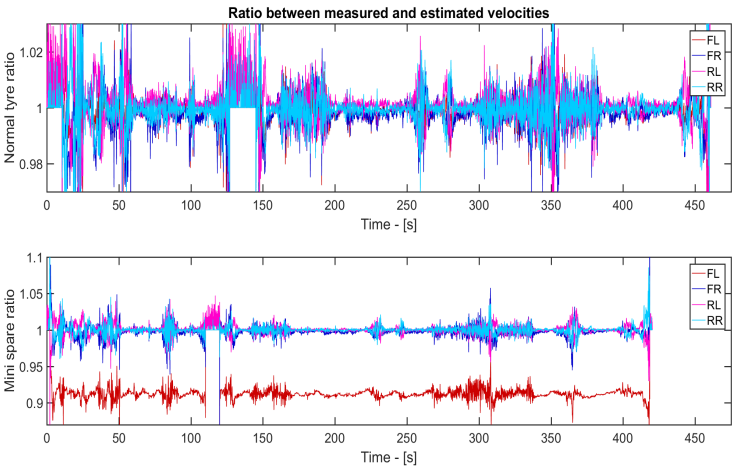

Figure B.12: Ratio for Test 1 during part 2 for normal tyres and minispare on FL

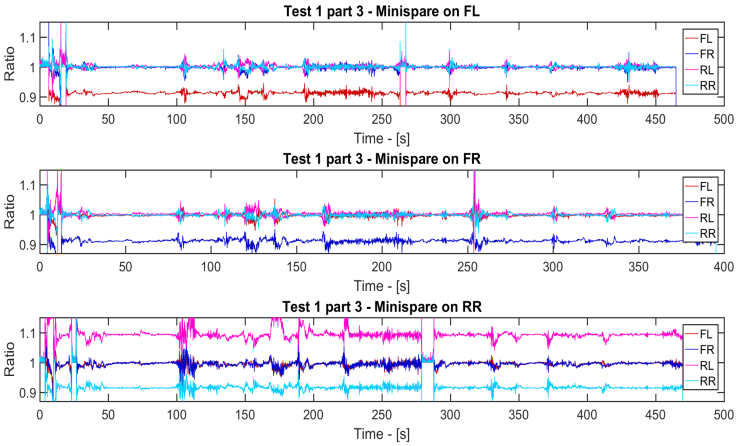

Figure B.13: Ratio for Test 1 during part 3 with minispare on FL, FR, and RR

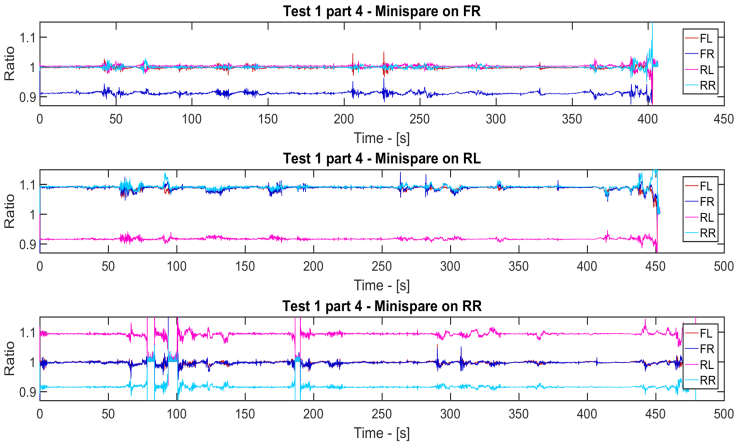

Figure B.14: Ratio for Test 1 during part 4 with minispare on FR, RL, and RR

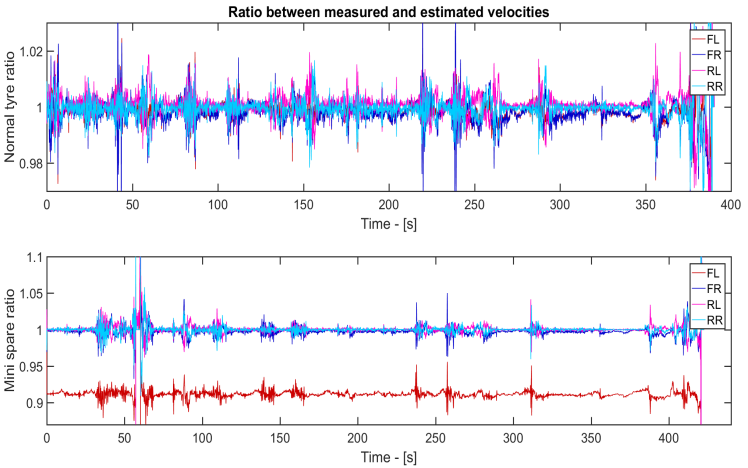

Figure B.15: Ratio for Test 1 during part 4 for normal tyres and minispare on FL

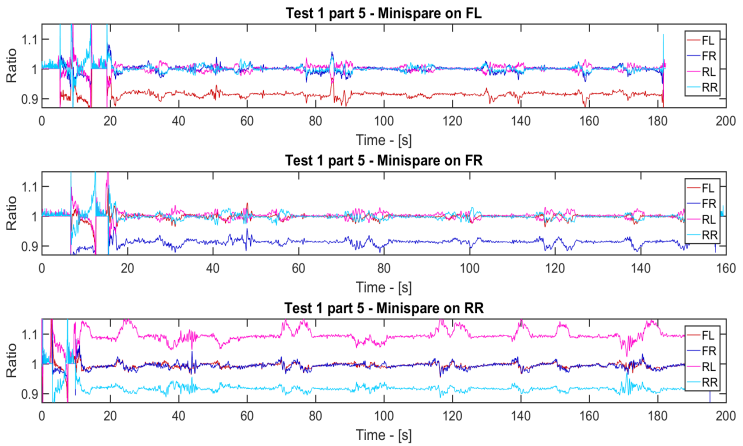

Figure B.16: Ratio for Test 1 during part 5 with minispare on FL, FR, and RR

Suspected and *Detected* for part 1-5

The *Suspected* and *Detected* are shown in table form, even the ones already presented in figures in chapter 8. They will provide the detection time, the number of times *Suspected* set to -1 and the number of times a wrong minispare was suspected. In these tables, Table B.6-B.10, all of the *Cannot decide* are the results from the vehicle standing still.

Part	Detection time	Nr. cannot decide	Nr. wrong suspected
1	20	9	0
2	35	7	0
3	30	5	0
4	20	1	0
5	40	3	0

Table B.6: Result from *Suspected* and *Detected* with normal tyres

Part	Detection time	Nr. cannot decide	Nr. wrong suspected
1	20	1	0
2	20	5	0
3	30	5	0
4	20	2	0
5	40	5	0

Table B.7: Result from *Suspected* and *Detected* with minispare on FL

Part	Detection time	Nr. cannot decide	Nr. wrong suspected
1	75	1	0
2	25	2	0
3	25	2	0
4	20	1	0
5	30	1	0

Table B.8: Result from *Suspected* and *Detected* with minispare on FR

Part	Detection time	Nr. cannot decide	Nr. wrong suspected
1	20	5	0
2	20	6	0
3	40	5	0
4	20	1	0
5	30	1	0

Table B.9: Result from *Suspected* and *Detected* with minispare on RL

Part	Detection time	Nr. cannot decide	Nr. wrong suspected
1	75	3	0
2	20	5	0
3	25	7	0
4	20	5	0
5	30	4	0

Table B.10: Result from *Suspected* and *Detected* with minispare on RR

C

Test 2 - Ljungbyhed

C.1 Algorithm 1

Ratios with minispare on rear left

This section provides the velocity ratio figures with a minispare on RL as well as tables showing *Suspected* and *Detected* from Test 2 using Algorithm 1, Table C.1-C.3. Note that the mean value of the FL and FR velocities is used for estimating the rear wheel speeds and that the mean value of the rear wheel velocities is used for estimating the front wheel speeds.

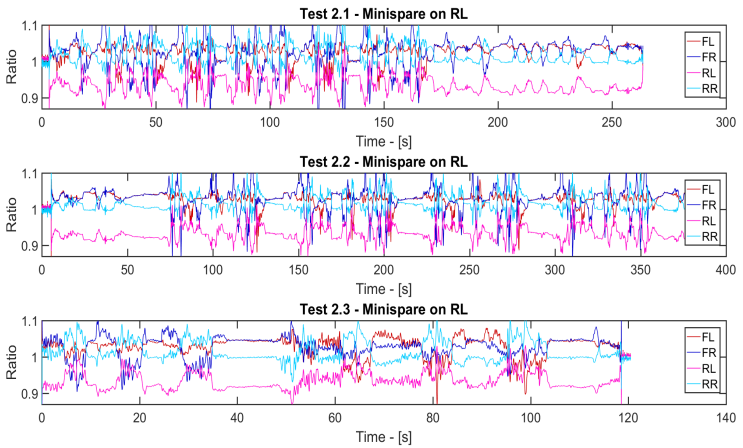

Figure C.1: Ratio for Test 2.1-2.3 with minispare on RL

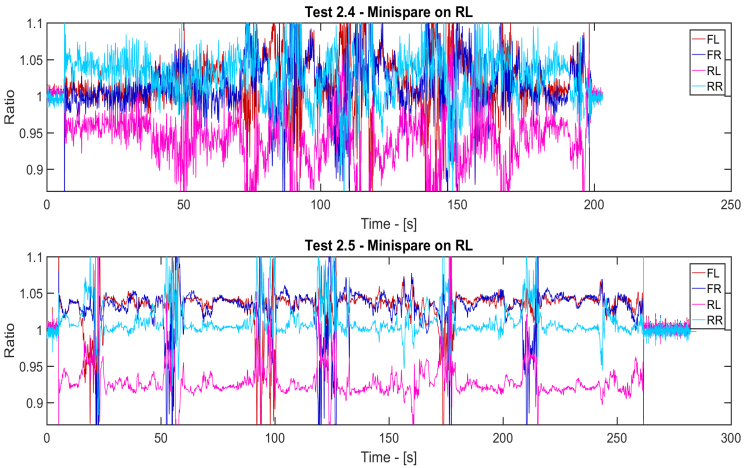

Figure C.2: Ratio for Test 2.4 and 2.5 with minispare on RL

Suspected and *Detected* for Test 2

The *Suspected* and *Detected* are shown in table form, even the ones already presented in figures in chapter 8. They will provide the detection time, the number of times *Suspected* set to -1 and the number of times a wrong minispare was suspected. In these tables, Table C.1-C.3, there will be a lot of *cannot decide*, this is because of the rough driving.

Test	Detection time	Nr. cannot decide	Nr. wrong suspected
2.1	25	19	0
2.2	20	21	0
2.3	60	9	0
2.4	25	20	9
2.5	20	15	0

Table C.1: Result from *Suspected* and *Detected* with normal tyres

Test	Detection time	Nr. cannot decide	Nr. wrong suspected
2.1	20	12	0
2.2	20	1	0
2.3	20	1	0
2.4	25	8	0
2.5	25	6	1

Table C.2: Result from *Suspected* and *Detected* with minispare on FL

Test	Detection time	Nr. cannot decide	Nr. wrong suspected
2.1	30	28	0
2.2	20	23	0
2.3	45	14	0
2.4	50	35	0
2.5	45	11	0

Table C.3: Result from *Suspected* and *Detected* with minispare on RL

C.2 Algorithm 2

This section provides the velocity ratio figures with a minispare on RL as well as tables showing *Suspected* and *Detected* from Test 2 using Algorithm 2. Note that the ratios are all from estimations based on RL except for the RL ratio that uses the RR estimation.

Ratios with minispare on rear left

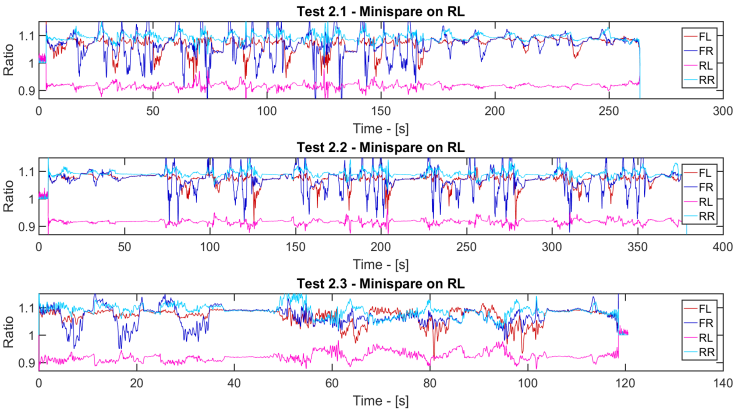

Figure C.3: Ratio for Test 2.1-2.3 with minispare on RL

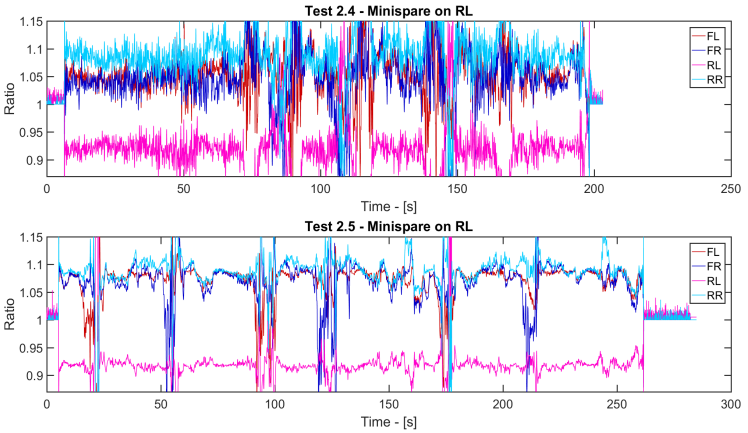

Figure C.4: Ratio for Test 2.4 and 2.5 with minispare on RL

Suspected and *Detected* for Test 2

The *Suspected* and *Detected* are shown in table form, even the ones already presented in figures in chapter 8. They will provide the detection time, the number of times *Suspected* set to -1 and the number of times a wrong minispare was suspected. In these tables, Table C.4-C.6, there will be a lot of *cannot decide*, this is because of the rough driving.

Test	Detection time	Nr. cannot decide	Nr. wrong suspected
2.1	55	28	0
2.2	20	27	0
2.3	20	7	0
2.4	20	23	6
2.5	20	18	0

Table C.4: Result from *Suspected* and *Detected* with normal tyres

Test	Detection time	Nr. cannot decide	Nr. wrong suspected
2.1	20	30	0
2.2	20	14	0
2.3	20	1	0
2.4	25	9	0
2.5	20	15	0

Table C.5: Result from *Suspected* and *Detected* with minispare on FL

Test	Detection time	Nr. cannot decide	Nr. wrong suspected
2.1	190	55	0
2.2	45	50	0
2.3	50	17	0
2.4	-	53	4
2.5	45	25	0

Table C.6: Result from *Suspected* and *Detected* with minispare on RL

D

Test 3 - City drive with Volvo XC40

D.1 Algorithm 1

This section provides all ratios, in Figure D.6-D.10, and tables showing the results from *Suspected* and *Detected*, in Table D.1-D.3, from Test 3 using Algorithm 1. It also shows the velocity estimation with a minispare on RR for all parts to explain the type of driving that was conducted. Note that the mean value of the FL and FR velocities is used for estimating the rear wheel speeds and the mean value of the rear velocities for the front speeds.

Velocity estimations and ratios with minispare on rear right

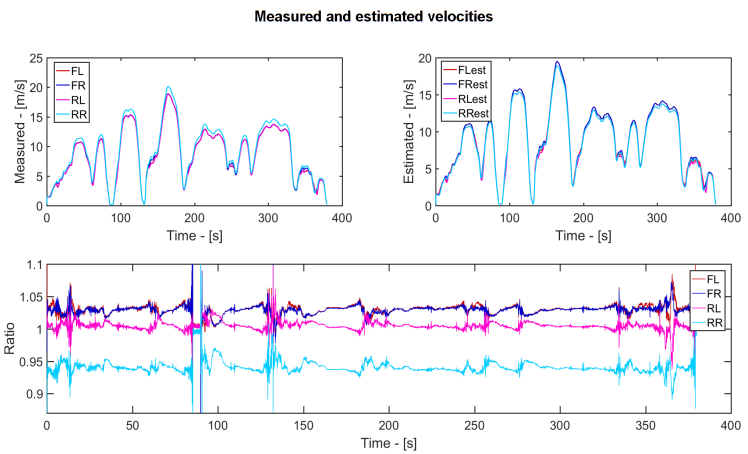

Figure D.1: Processed data from part 1 of Test 3 with minispare on RR

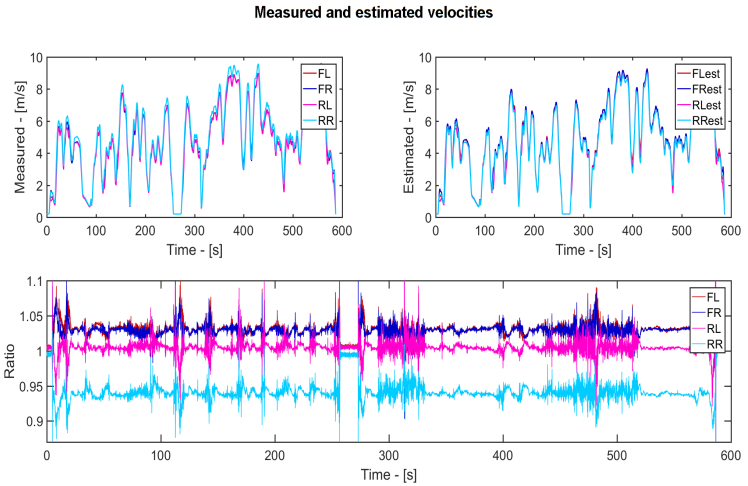

Figure D.2: Processed data from part 2 of Test 3 with minispare on RR

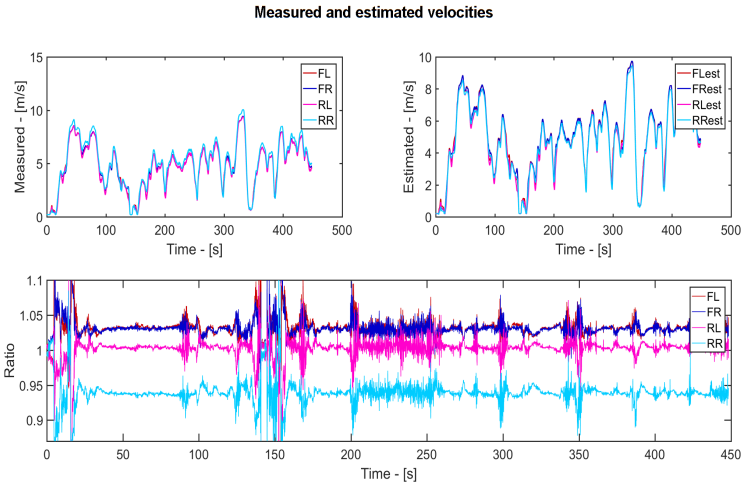

Figure D.3: Processed data from part 3 of Test 3 with minispare on RR

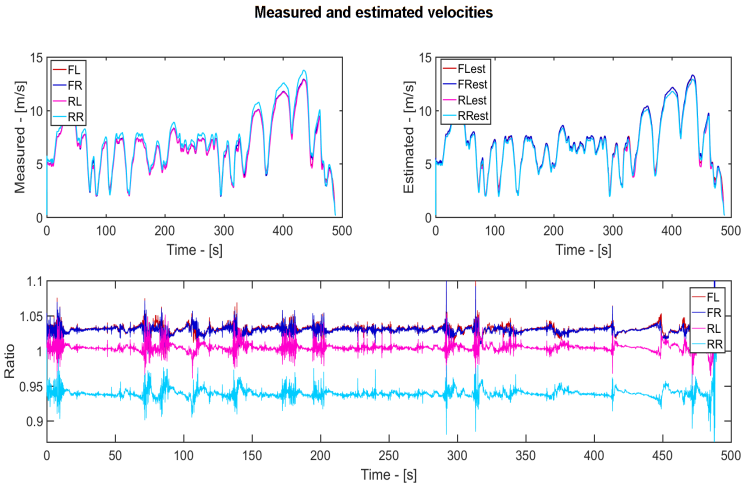

Figure D.4: Processed data from part 4 of Test 3 with minispare on RR

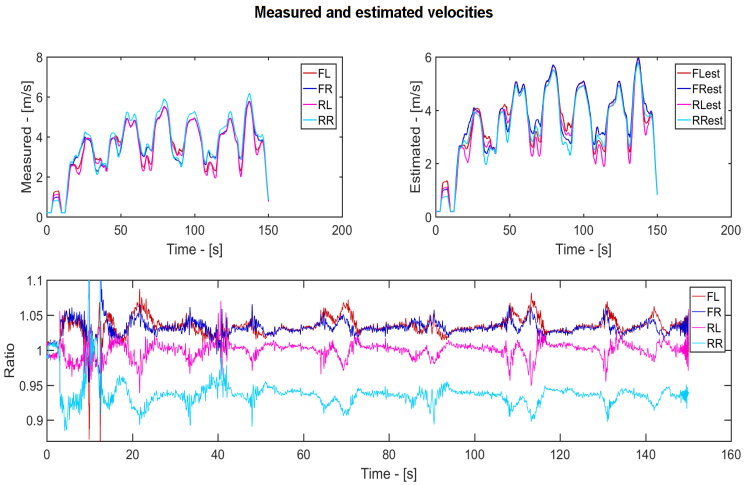

Figure D.5: Processed data from part 5 of Test 3 with minispare on RR

Ratio with normal tyres and minispare on front right

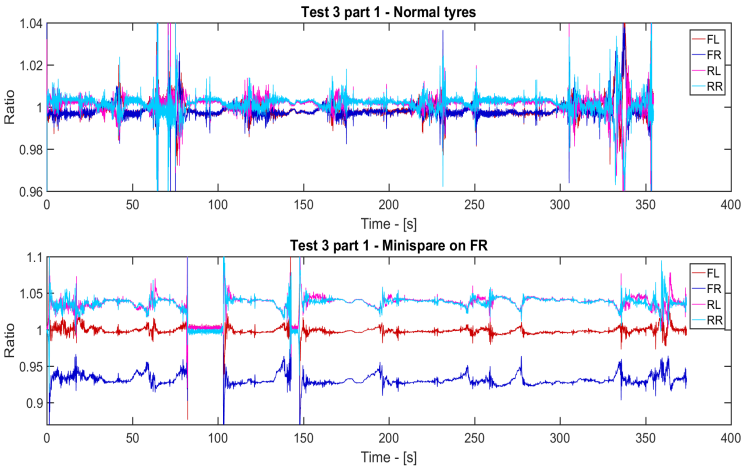

Figure D.6: Ratio for Test 3 part 1 for normal tyres and minispare on FR

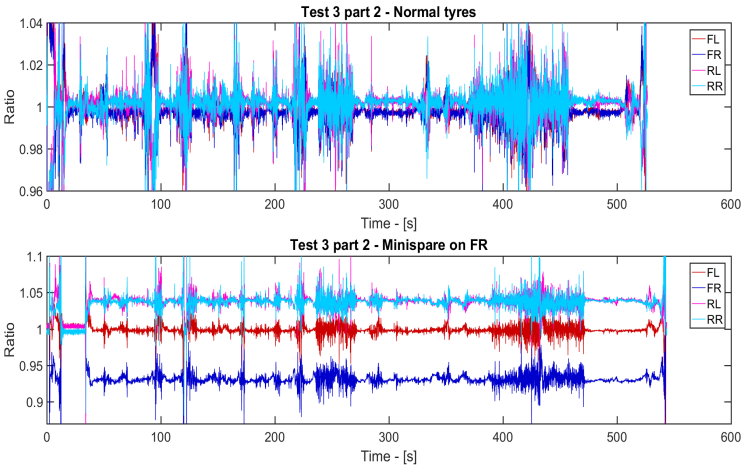

Figure D.7: Ratio for Test 3 part 2 for normal tyres and minispare on FR

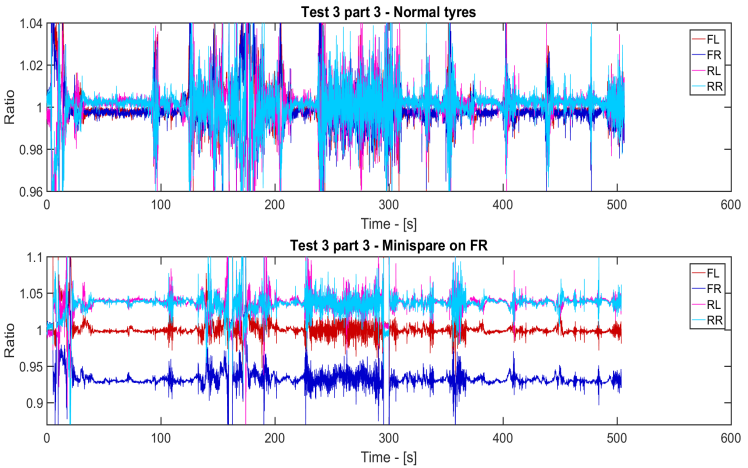

Figure D.8: Ratio for Test 3 part 3 for normal tyres and minispare on FR

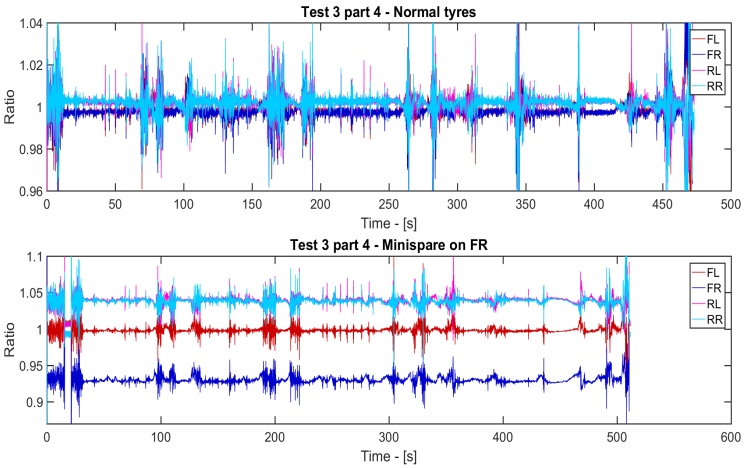

Figure D.9: Ratio for Test 3 part 4 for normal tyres and minispare on FR

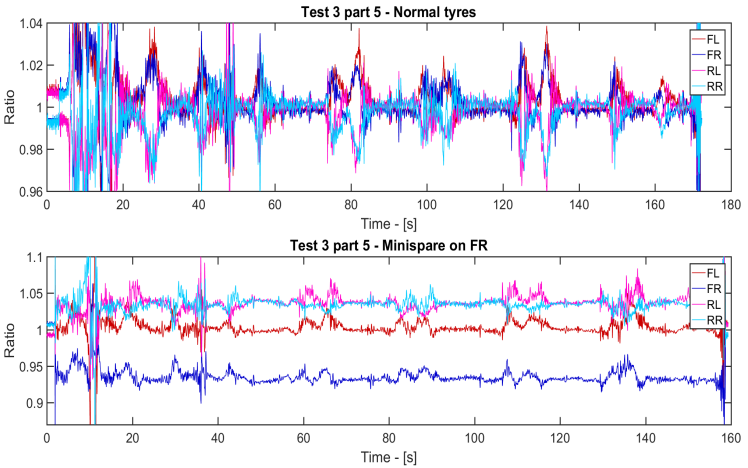

Figure D.10: Ratio for Test 3 part 5 for normal tyres and minispare on FR

Suspected and *Detected* for Test 3

The *Suspected* and *Detected* are shown in table form, even the ones already presented in figures in chapter 8. They will provide the detection time, the number of times *Suspected* set to -1 and the number of times a wrong minispare was suspected. In these tables, Table D.1-D.3, some of the *cannot decide* are due to the vehicle standing still.

Part	Detection time	Nr. cannot decide	Nr. wrong suspected
1	20	9	0
2	25	10	0
3	25	16	0
4	20	2	0
5	40	11	0

Table D.1: Result from *Suspected* and *Detected* with normal tyres

Part	Detection time	Nr. cannot decide	Nr. wrong suspected
1	20	8	0
2	45	7	0
3	25	8	0
4	20	2	0
5	20	1	0

Table D.2: Result from *Suspected* and *Detected* with minispare on FR

Part	Detection time	Nr. cannot decide	Nr. wrong suspected
1	20	7	0
2	25	9	0
3	25	11	0
4	20	2	0
5	25	7	0

Table D.3: Result from *Suspected* and *Detected* with minispare on RR

D.2 Algorithm 2

This section provides all Ratio figures, Figure D.11-D.15 and the *Suspected* and *Detected* tables, Table D.4-D.6. Note that the ratios are all from estimations based on rear left except for the RL ratio that uses the rear right estimation.

Ratios with normal tyres and minispare on front right and rear right

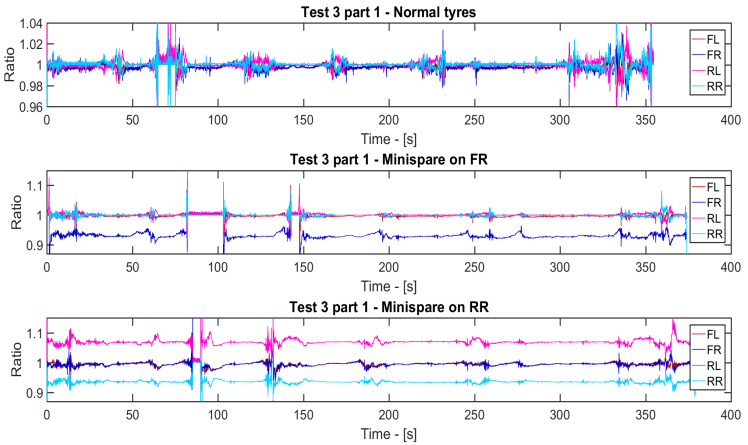

Figure D.11: Ratio for Test 3 part 1 with normal tyres, minispare on FR and RR

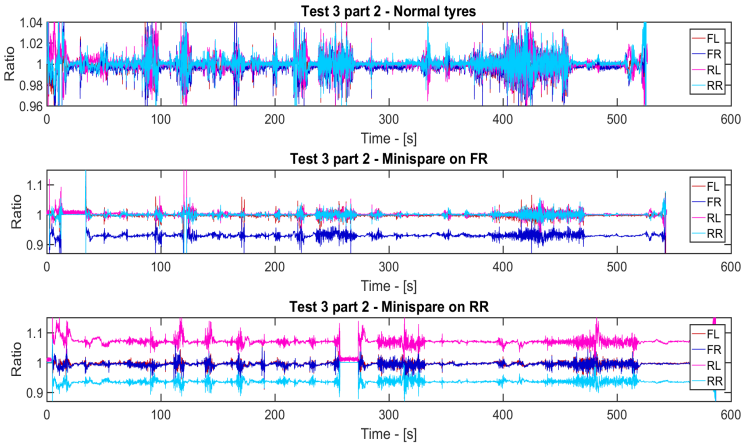

Figure D.12: Ratio for Test 3 part 2 with normal tyres, minispare on FR and RR

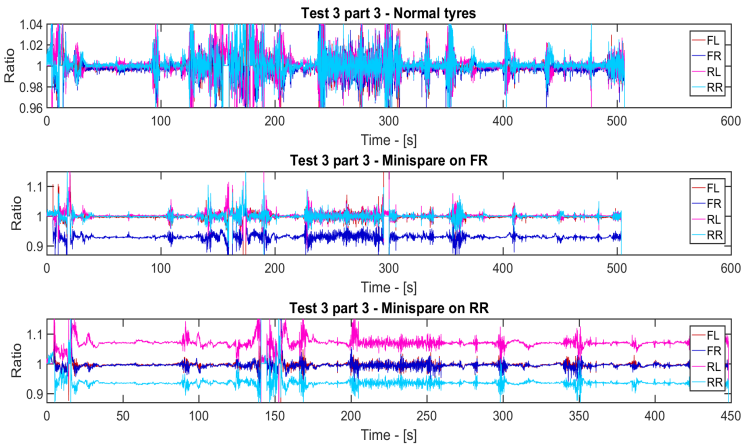

Figure D.13: Ratio for Test 3 part 3 with normal tyres, minispare on FR and RR

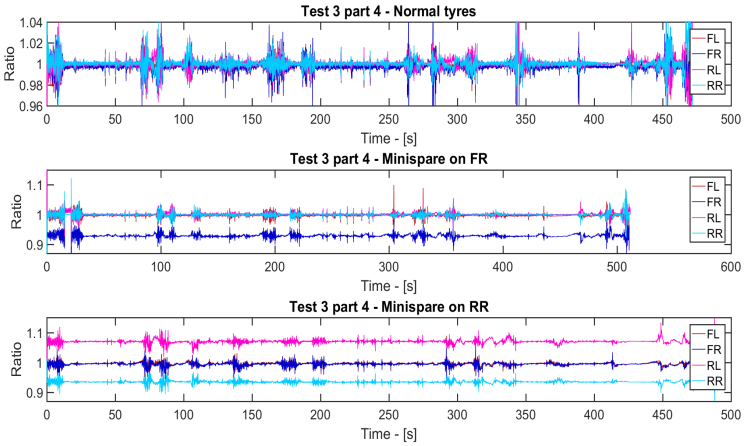

Figure D.14: Ratio for Test 3 part 4 with normal tyres, minispare on FR and RR

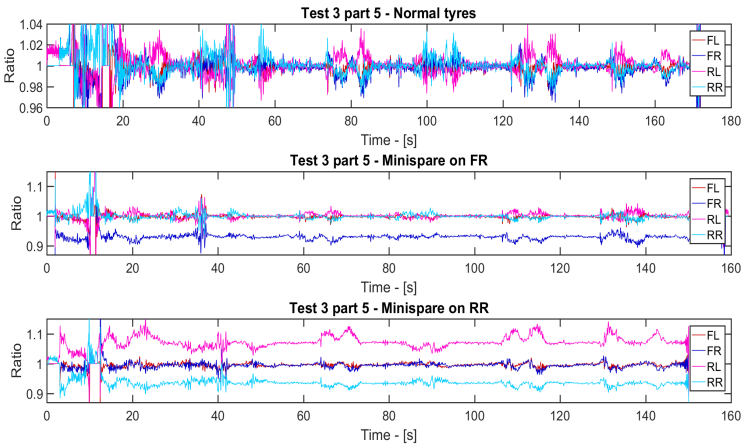

Figure D.15: Ratio for Test 3 part 5 with normal tyres, minispare on FR and RR

Suspected and *Detected* for Test 3

The *Suspected* and *Detected* are shown in table form, even the ones already presented in figures in chapter 8. They will provide the detection time, the number of times *Suspected* set to -1 and the number of times a wrong minispare was suspected. In these tables, Table D.4-D.6, some of the *cannot decide* are due to the vehicle standing still.

Part	Detection time	Nr. cannot decide	Nr. wrong suspected
1	20	9	0
2	25	6	0
3	25	15	0
4	20	1	0
5	30	5	0

Table D.4: Result from *Suspected* and *Detected* with normal tyres

Part	Detection time	Nr. cannot decide	Nr. wrong suspected
1	20	7	0
2	50	7	0
3	25	9	0
4	20	2	0
5	25	2	0

Table D.5: Result from *Suspected* and *Detected* with minispare on FR

Part	Detection time	Nr. cannot decide	Nr. wrong suspected
1	20	10	0
2	20	8	0
3	25	4	0
4	20	1	0
5	25	5	1

Table D.6: Result from *Suspected* and *Detected* with minispare on RR

E

Radius estimation

In this appendix, the radius estimations for all the tests and their respective cases is presented. The results from Test 1 is shown in Figure E.3-E.11, Test 2 in Figure E.12-E.17 and Test 3 in Figure E.18-E.23. One thing to note in every figure is that the blue line will always represent *approximated* or *decided* radius depending on which figure it is while the red line is the actual radius of the minispare. Algorithm 1 will be presented in the left of the figures and Algorithm 2 to the right.

E.1 Test 1 - City drive

Minispare on front left

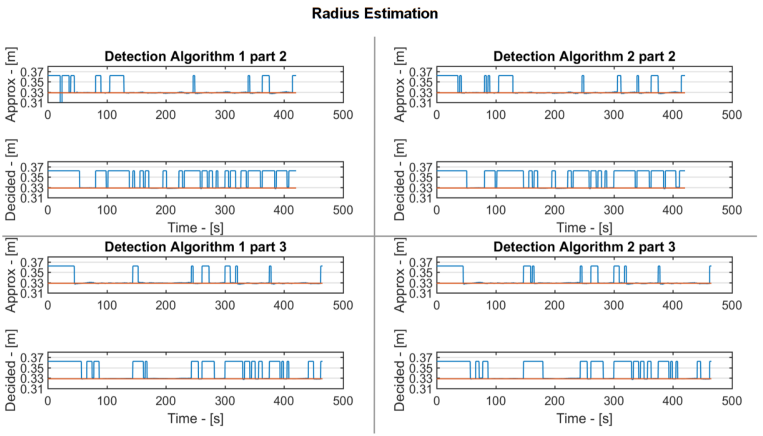

Figure E.1: Approximated and decided radius for part 2 and 3 with minispare on FL

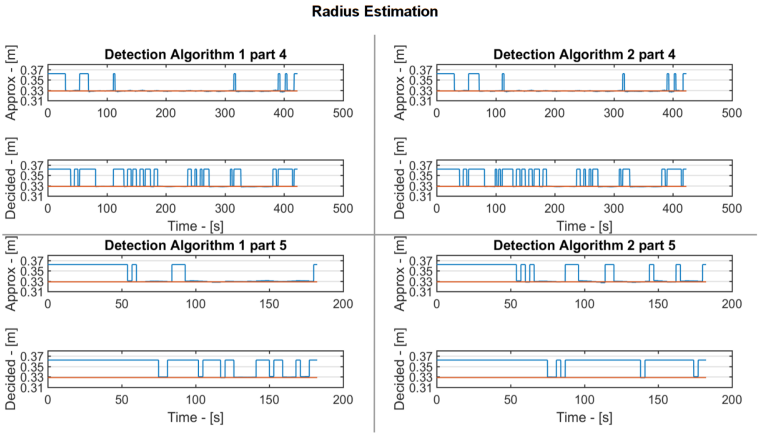

Figure E.2: Approximated and decided radius for part 4 and 5 with minispare on FL

Minispare on front right

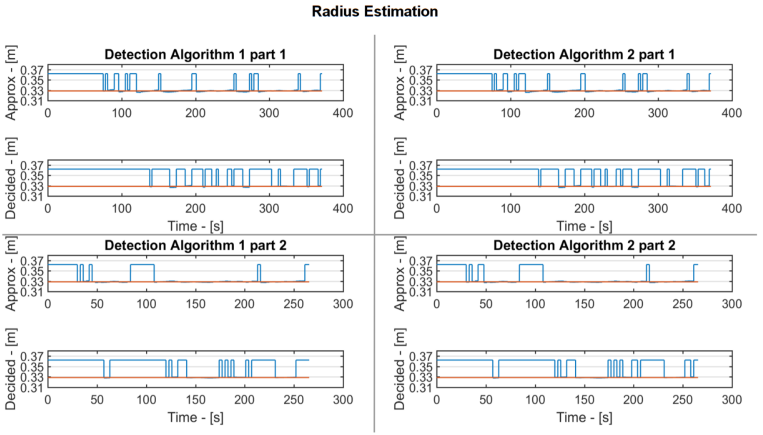

Figure E.3: Approximated and decided radius for part 1 and 2 with minispare on FR

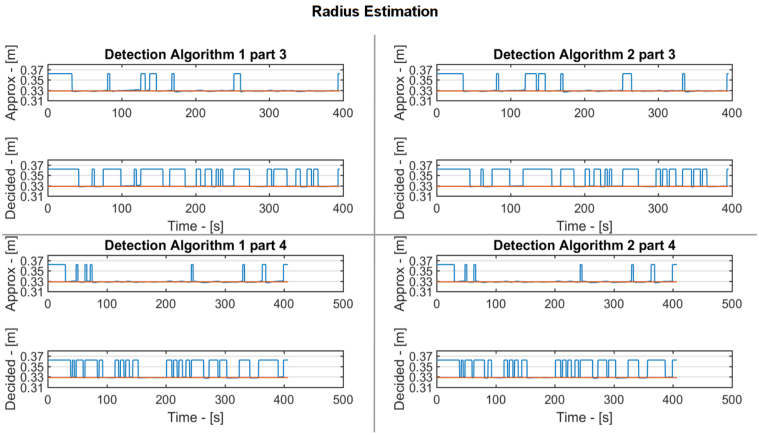

Figure E.4: Approximated and decided radius for part 3 and 4 with minispare on FR

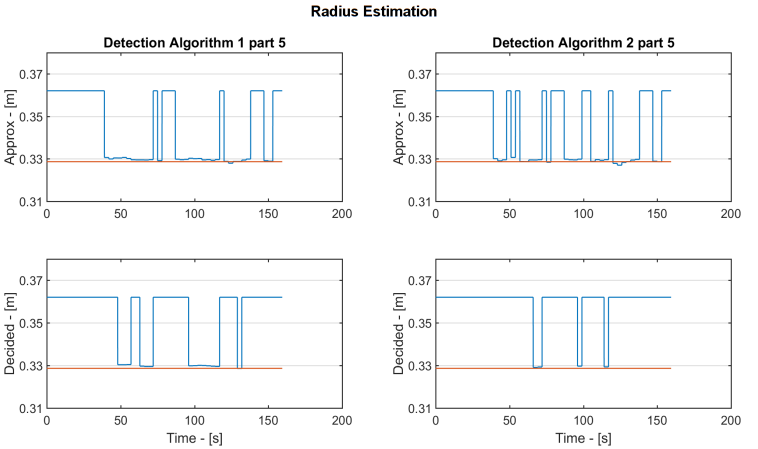

Figure E.5: Approximated and decided radius for part 5 with minispare on FR

Minispare on rear left

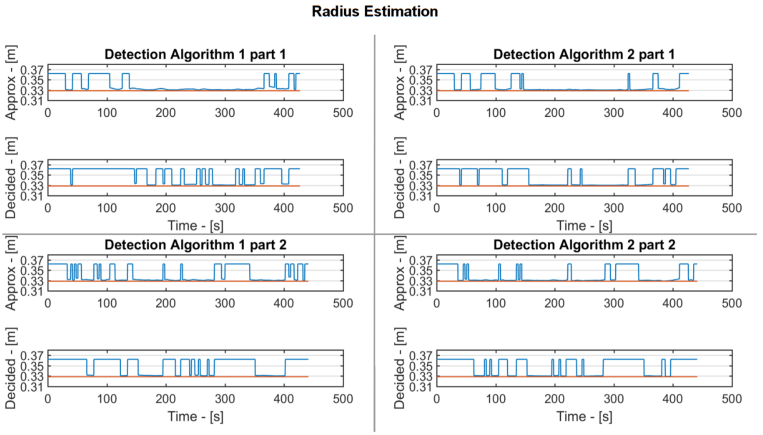

Figure E.6: Approximated and decided radius for part 1 and 2 with minispare on RL

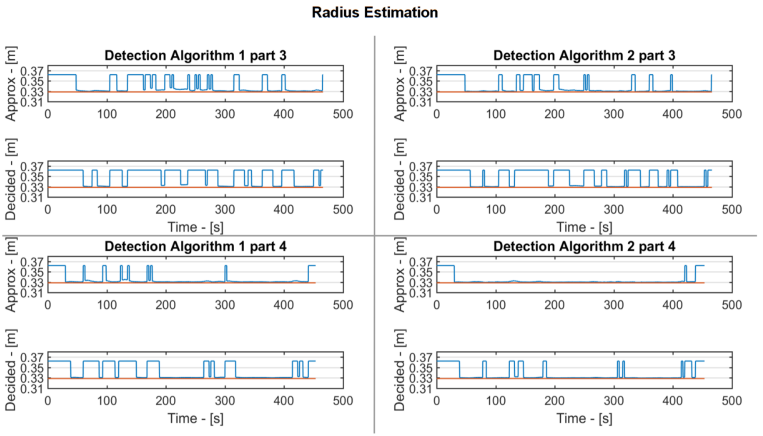

Figure E.7: Approximated and decided radius for part 3 and 4 with minispare on RL

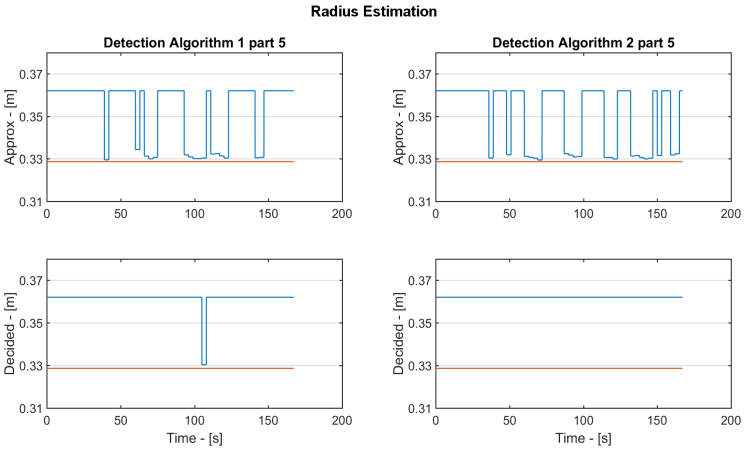

Figure E.8: Approximated and decided radius for part 5 with minispare on RL

Minispare on rear right

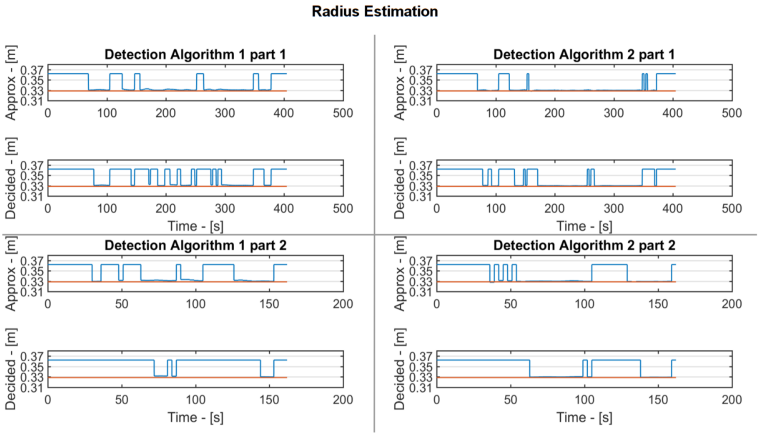

Figure E.9: Approximated and decided radius for part 1 and 2 with minispare on RR

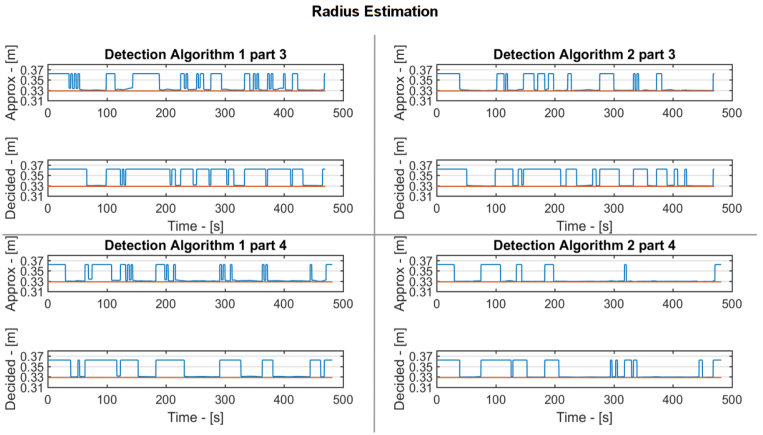

Figure E.10: Approximated and decided radius for part 3 and 4 with minispare on RR

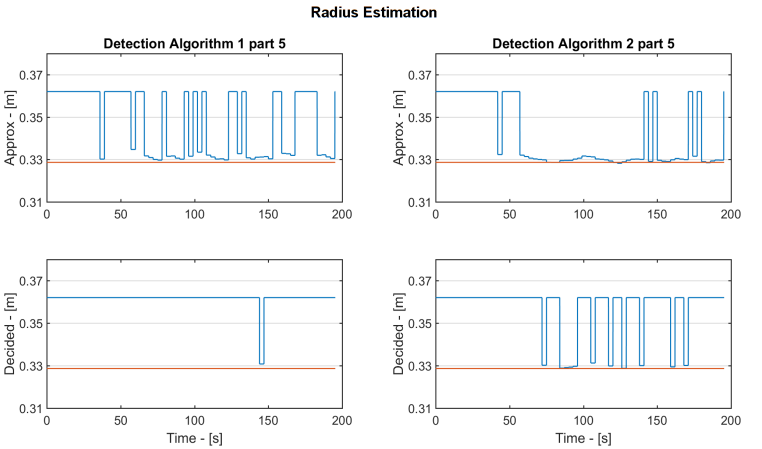

Figure E.11: Approximated and decided radius for part 5 with minispare on RR

E.2 Test 2 - Ljungbyhed

Minispare on front left

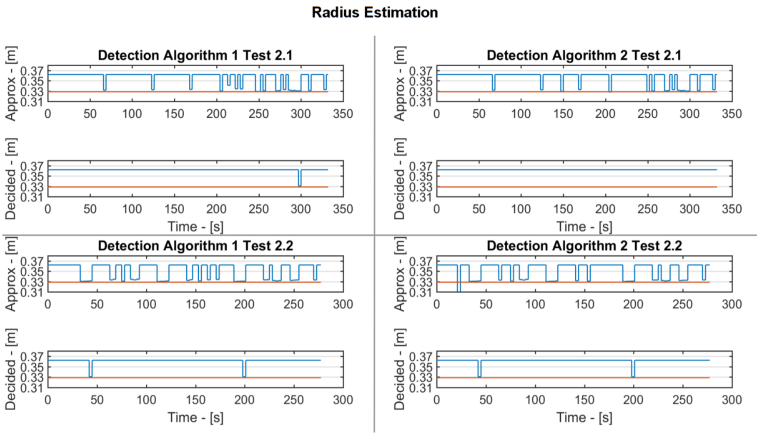

Figure E.12: Approximated and decided radius for Test 2.1 and 2.2 with minispare on FL

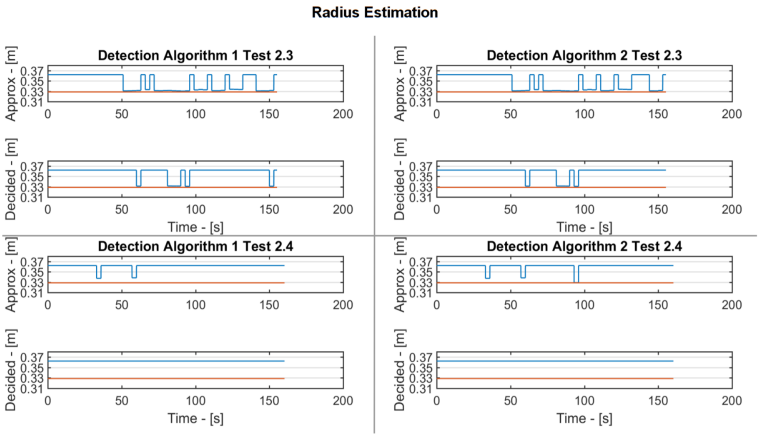

Figure E.13: Approximated and decided radius for Test 2.3 and 2.4 with minispare on FL

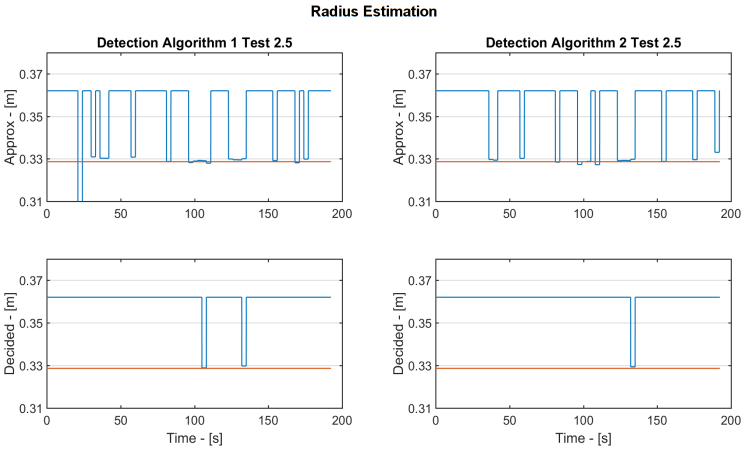

Figure E.14: Approximated and decided radius for Test 2.5 with minispare on FL

Minispare on rear left

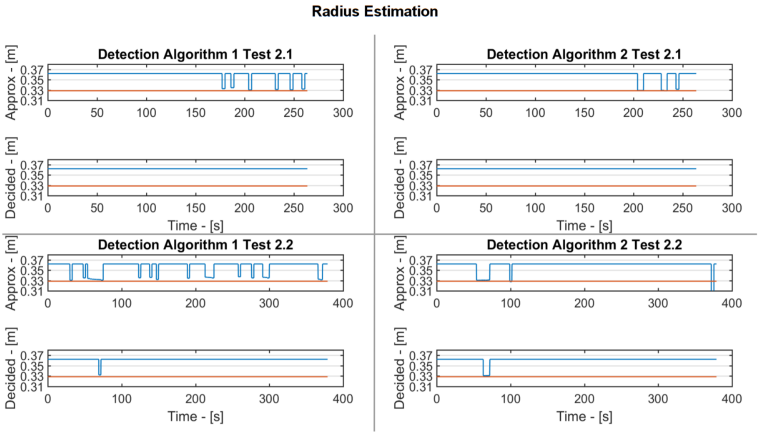

Figure E.15: Approximated and decided radius for Test 2.1 and 2.2 with minispare on RL

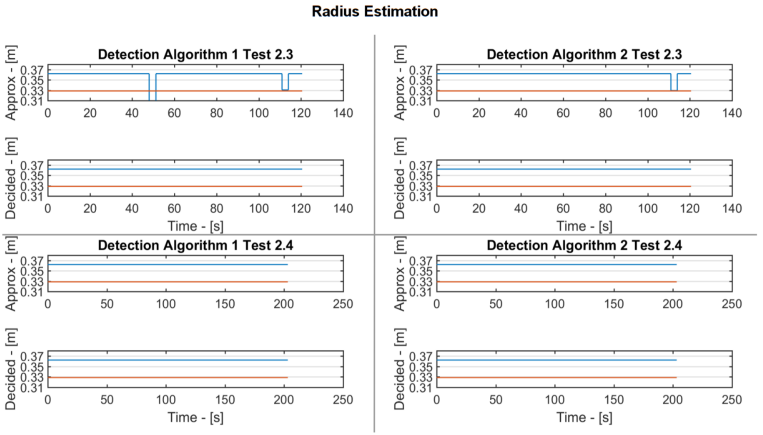

Figure E.16: Approximated and decided radius for Test 2.3 and 2.4 with minispare on RL

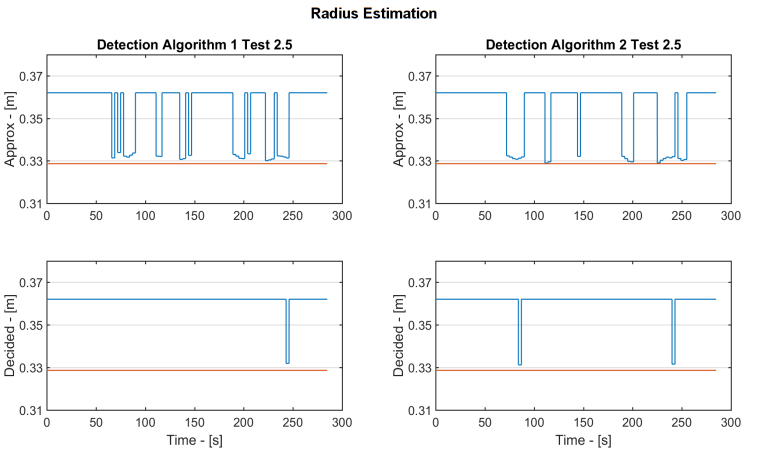

Figure E.17: Approximated and decided radius for Test 2.5 with minispare on RL

E.3 Test 3 - City drive with XC40

Minispare on front right

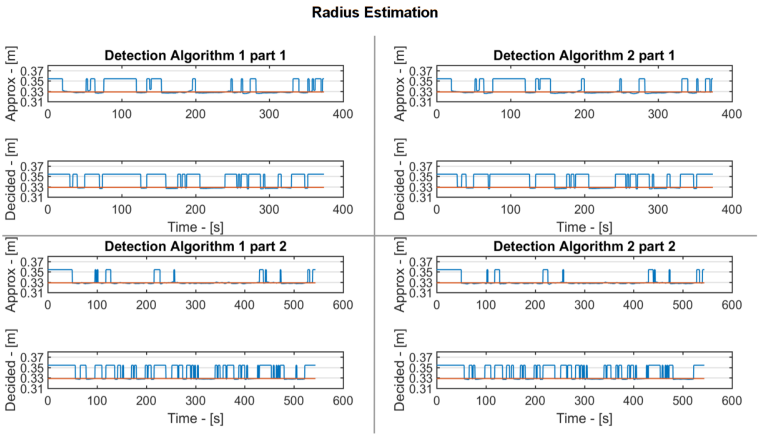

Figure E.18: Approximated and decided radius for part 1 and 2 with minispare on FR

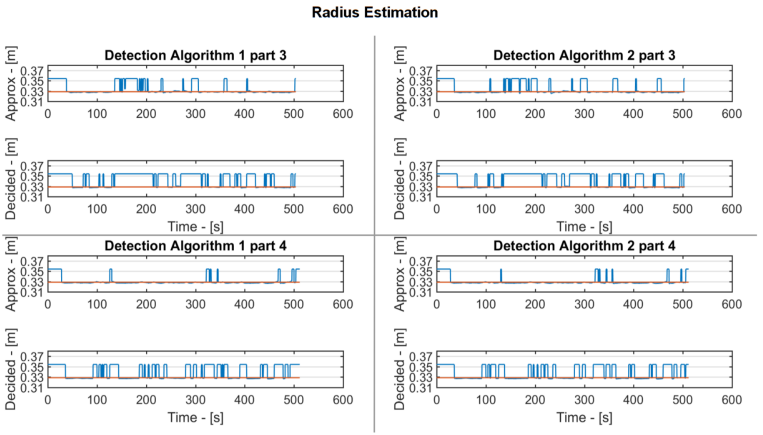

Figure E.19: Approximated and decided radius for part 3 and 4 with minispare on FR

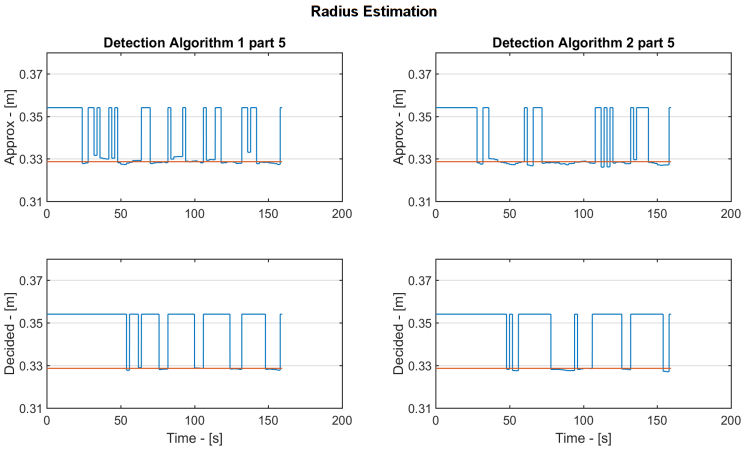

Figure E.20: Approximated and decided radius for part 5 with minispare on FR

Minispare on rear right

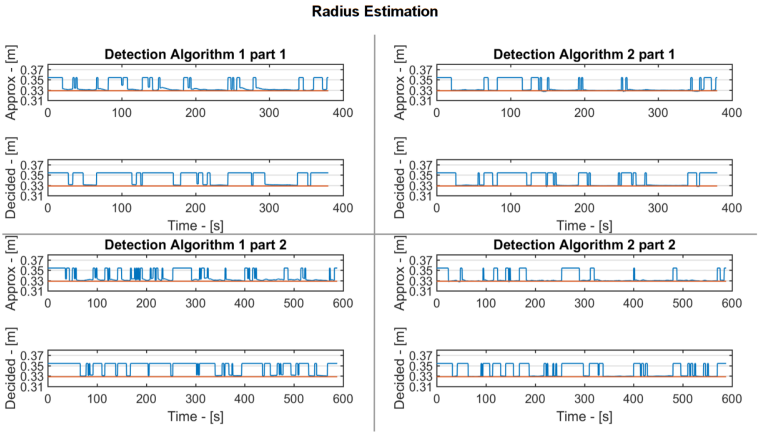

Figure E.21: Approximated and decided radius for part 1 and 2 with minispare on RR

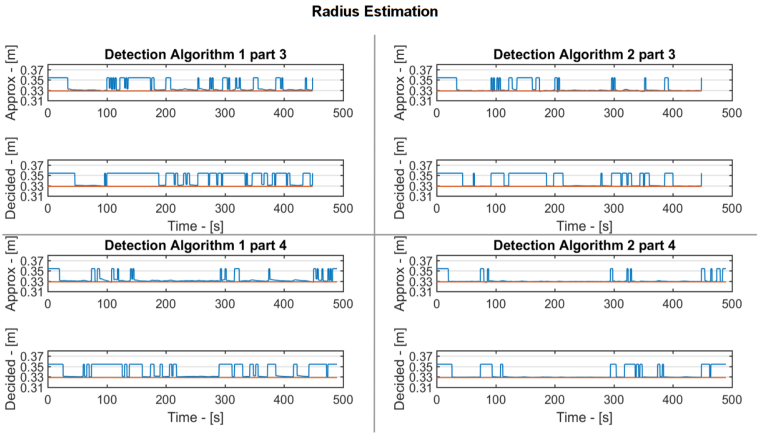

Figure E.22: Approximated and decided radius for part 3 and 4 with minispare on RR

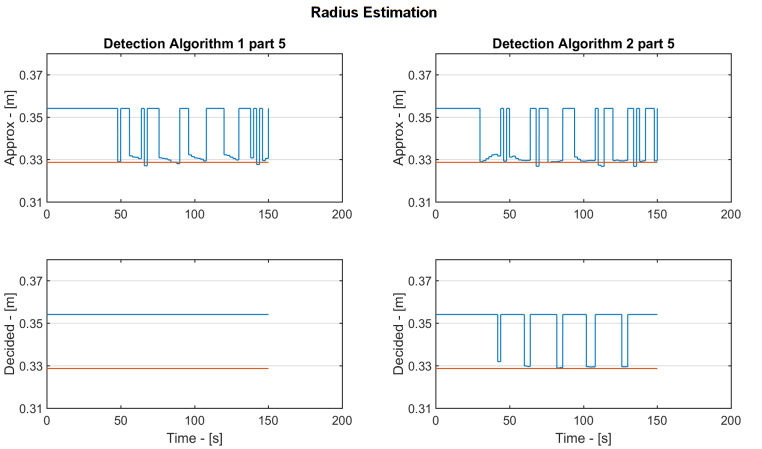

Figure E.23: Approximated and decided radius for part 5 with minispare on RR

Lund University
Department of Automatic Control
Box 118
SE-221 00 Lund Sweden

Document name
MASTER'S THESIS

Date of issue
June 2021

Document Number
TFRT-6145

Author(s)
Isabella Hansen
Johanna Wikström

Supervisor
Ola Nicklasson, BorgWarner, Sweden
Tore Hägglund, Dept. of Automatic Control, Lund University, Sweden
Anton Cervin, Dept. of Automatic Control, Lund University, Sweden (examiner)

Title and subtitle
Enhanced Detection of Minispare Usage

Abstract

Minispares, or spare wheels, can often cause a lot of problems for the control of the car since it rotates notably faster than normal tyres. This because it is often smaller to reduce weight. When a minispare is used, it needs to be detected for the control system to understand that one tyre is allowed to spin faster compared to the others. If the control system does not know this, it will believe that the wheel is slipping and therefore, slow down the speed of the tyre. This detection must happen fast so that the driving experience is affected as little as possible.

This project consisted of improving an already existing method that BorgWarner currently uses to detect minispare usage. The main goal was to decrease the detection time to enhance the driving experience. To reach this goal, different detection algorithms were created and validated with various tests. The algorithms were all based on estimations of the tyres' velocities which were then compared to the measured velocities. In the end, two algorithms were presented which could detect a minispare usage, and the lack of it, in a satisfactory time.

Keywords

Classification system and/or index terms (if any)

Supplementary bibliographical information

ISSN and key title
0280-5316

ISBN

Language
English

Number of pages
1-110

Recipient's notes

Security classification

http://www.control.lth.se/publications/